



Two dimensional laser-collision induced fluorescence measurements in low pressure plasmas

**15th International Symposium on
Laser-Aided Plasma Diagnostics (LAPD)
Jeju, Korea, October 9'th - 13'th 2011**

Edward V. Barnat, Brandon Weatherford and Kraig Frederickson

**Sandia National Laboratories
Albuquerque, N.M., United States of America**

*This work was supported by the Department of Energy Office of Fusion Energy Science
Contract DE-SC0001939*

Sandia is a multiprogram laboratory operated by Sandia Corporation, a Lockheed Martin Company, for the United States Department of Energy's National Nuclear Security Administration under contract DE-AC04-94AL85000.



LOCKHEED MARTIN 



Sandia National Laboratories

Laser-collision induced fluorescence provides measure of electron density and "temperature"

- **Motivation: What is the density? What is the temperature? Where and When?**
 - More traditional probe techniques may couple and perturb
 - Optically passive techniques are line-of-sight limited
 - Optically active-techniques such as Thomson scattering pose their own set of challenges
- **In this presentation**
 - Laser-collision induced fluorescence (LCIF) primer
 - Collisional-radiative model used to predict LCIF
 - Applied to triplet manifold of Helium
 - Implement and benchmark technique
 - Experimental setup
 - Time evolution of LCIF and time integrated LCIF
 - Applications of LCIF:
 - Ion sheaths, transient double layers, positive columns
 - Future directions and concluding comments
 - Extension of helium
 - Investigate argon



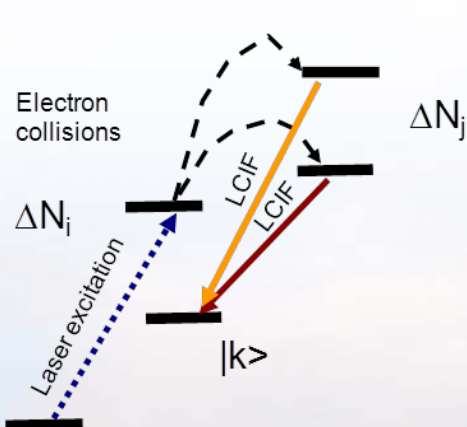
Sandia National Laboratories

Part I: LCIF concepts and key trends

■ Overview

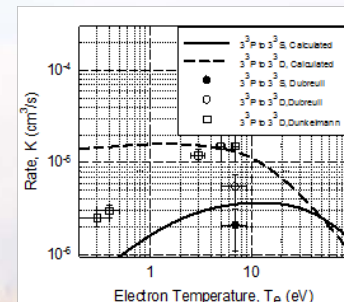
- LCIF concepts
- Collisional-radiative model for helium
- Key scaling trends

LCIF Concept

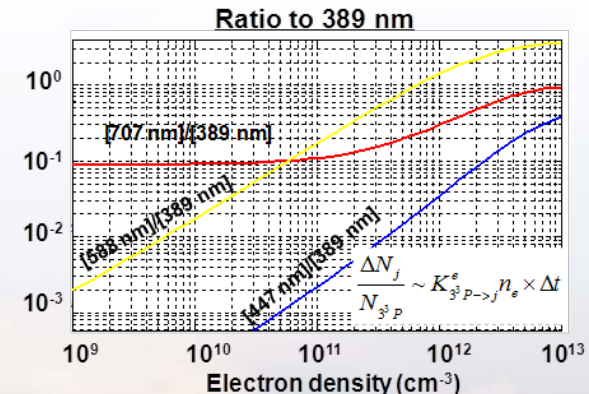


CR Model

$$\frac{dN_j}{dt} = \left[\sum_{i \neq j} K_{ij}^e N_i - \sum_{i \neq j} K_{ji}^e N_j \right] n_e + \dots$$



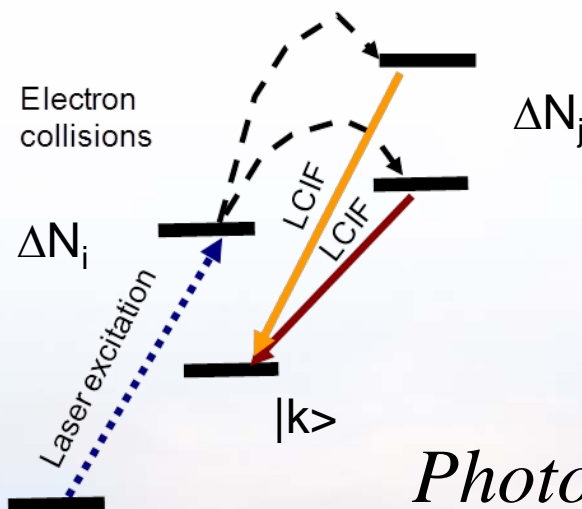
Key scaling trends





LCIF is based on redistribution of excited state by plasma electrons

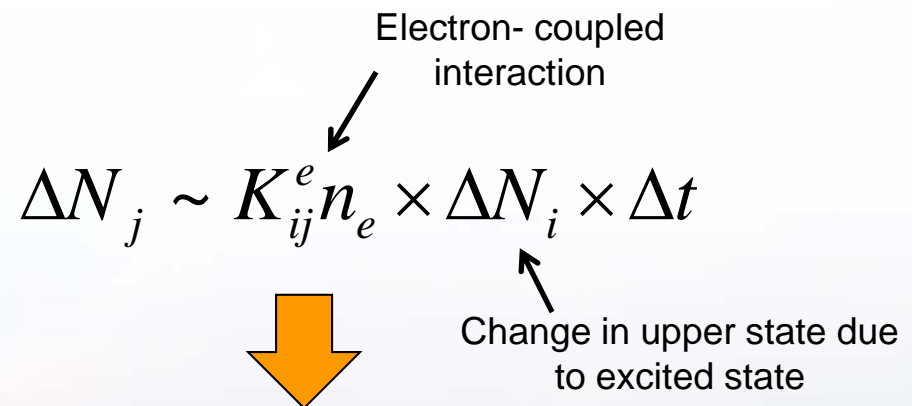
- Laser excitation causes populates an intermediate state
 - Relaxation processes deplete excited state
- Portion of excited state population gets redistributed into "uphill" states
 - Driven by interaction with energetic plasma electrons



Electron- coupled interaction

$$\Delta N_j \sim K_{ij}^e n_e \times \Delta N_i \times \Delta t$$

Change in upper state due to excited state



Equation for LCIF population change:

$$\Delta N_j \sim K_{ij}^e n_e \times \Delta N_i \times \Delta t$$

Photons emitted $\sim A_{jk} \times \Delta N_j \times \Delta t$ Detected light

LCIF looks for changes in emission of neighboring states after laser excitation





Redistribution after laser excitation is complex

- A "good" model is required to predict transfer between levels
 - Employ a collisional-radiative model (CRM) to predict redistribution

$$\frac{dN_j}{dt} = \left[\sum_{i \neq j} K_{ij}^e N_i - \sum_{i \neq j} K_{ji}^e N_j \right] n_e + \left[\sum_{i > j} A_{ij} N_i - \sum_{i < j} A_{ji}^j N_j \right] + \sum_k \left[\sum_{i \neq j} K_{ikj}^a N_i - \sum_{i \neq j} K_{jki}^a N_j \right] N_k$$

- Electron density and electron temperature appear in first term
 - Temperature dependence introduced via K_{ij}^e

Electron-temperature dependent rates

$$K_{ij}^e = \left\langle \sigma_{ij}(E) v_e \right\rangle$$

Distribution function used for describing electron velocities

$$f(v) \sim e^{\frac{(\frac{1}{2}mv)^2}{kT}}$$

Approach is applicable to various atomic and molecular systems of interest

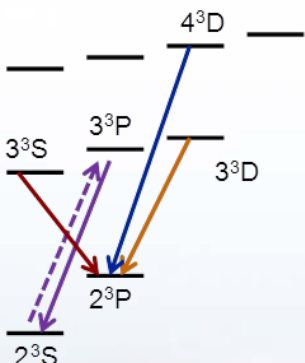




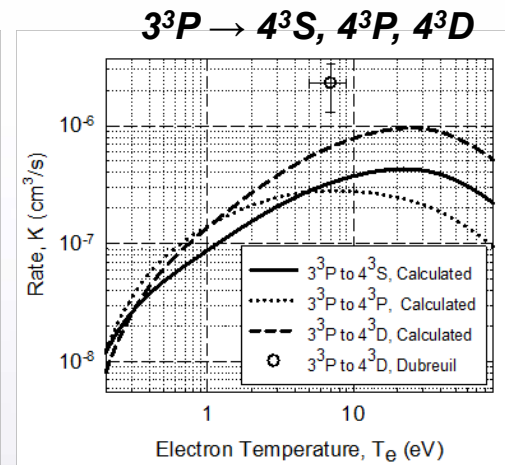
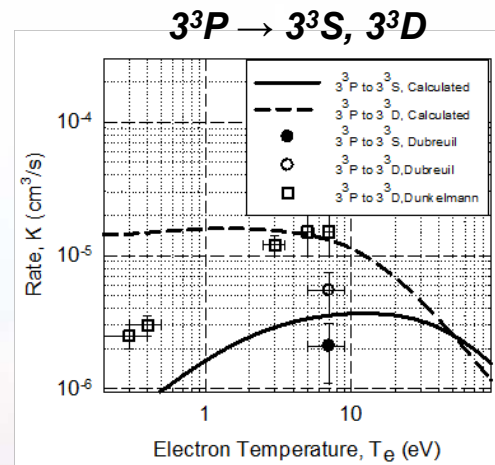
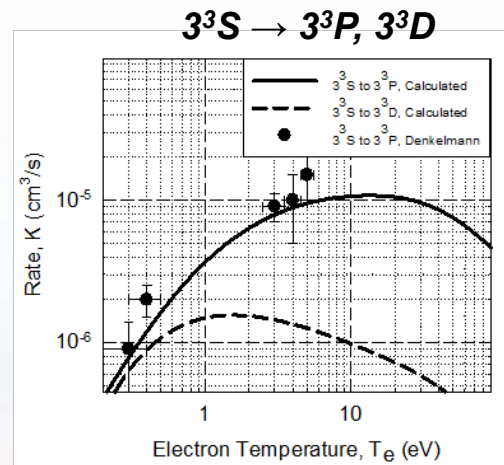
Helium atom serves as target species for LCIF measurements

- Employ Helium to start with - considering argon
 - "Simple system" with "better known" rates
- Utilize functionalized form of cross-sections compiled by Ralchenko¹
 - Integrate to get rates, compare to measured rates ^{2,3}

Key transitions



Computed and measured excitation rates in Helium



1: Yu. Ralchenko, R. K. Janev, T. Kato, D. V. Fursa, I. Bray, F. J. De Heer, Atomic Data and Nuclear Data Tables **94**, 603 (2008)

2: R. Denkelmann, S. Maurmann, T. Lokajczyk, P. Drepper, and H. -J. Kunze, J. Phys. B: At. Mol. Opt. Phys. **32**, 4635 (1999).

R. Denkelmann, S. Freund and S. Maurmann, Contrib. Plasma Phys. **40**, 91 (2000).

3: B. Dubreuil and P. Prigent, J. Phys. B: At. Mol. Opt. Phys. **18**, 4597 (1985).



Accuracy of n_e , T_e depend on knowledge of $K_{ij}(kT_e)$

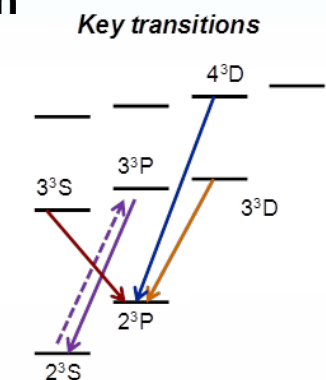


Sandia National Laboratories

CRM predicts evolution of various helium states after laser excitation

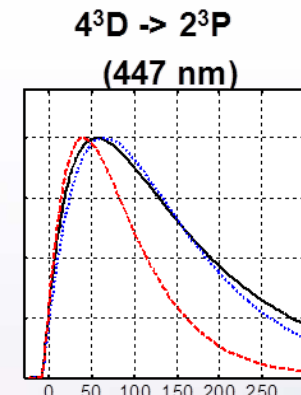
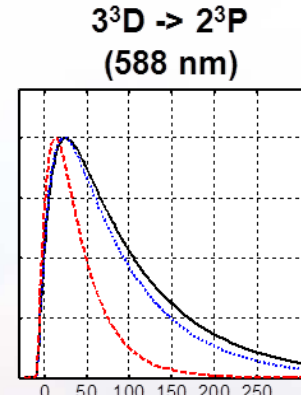
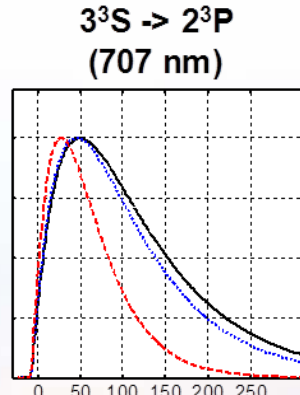
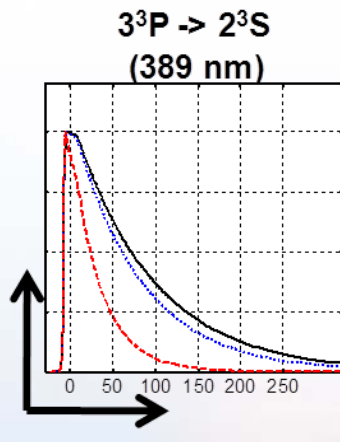
- Temporal evolution serves as a partial "fingerprint" of electron interaction
 - Analyze shape of decay above $n_e \sim 10^{11}$ electrons/cm³
 - Below $n_e \sim 10^{11}$ absolute intensities are needed

$$K_{ij}^e n_e \sim A_{ij} \quad \rightarrow \quad 10^{-5} \times 10^{11} \sim 10^7$$



Computed temporal evolution

Normalized LCIF



$n_e = 10^{10} \text{ e/cm}^3$
 $n_e = 10^{11} \text{ e/cm}^3$
 $n_e = 10^{12} \text{ e/cm}^3$

$kT_e = 2 \text{ eV}$

Need at least two time-resolved profiles to uniquely obtain n_e , kT_e

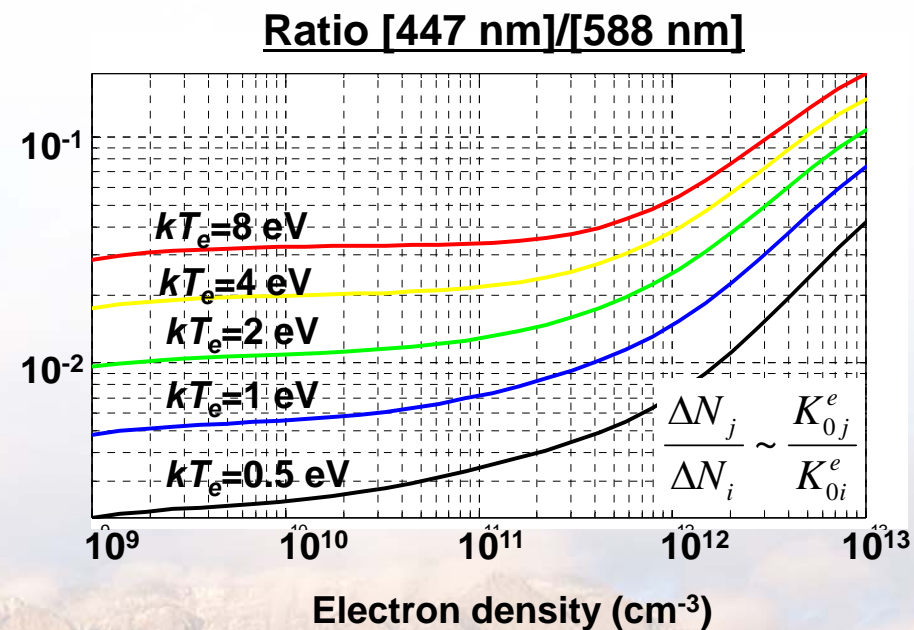
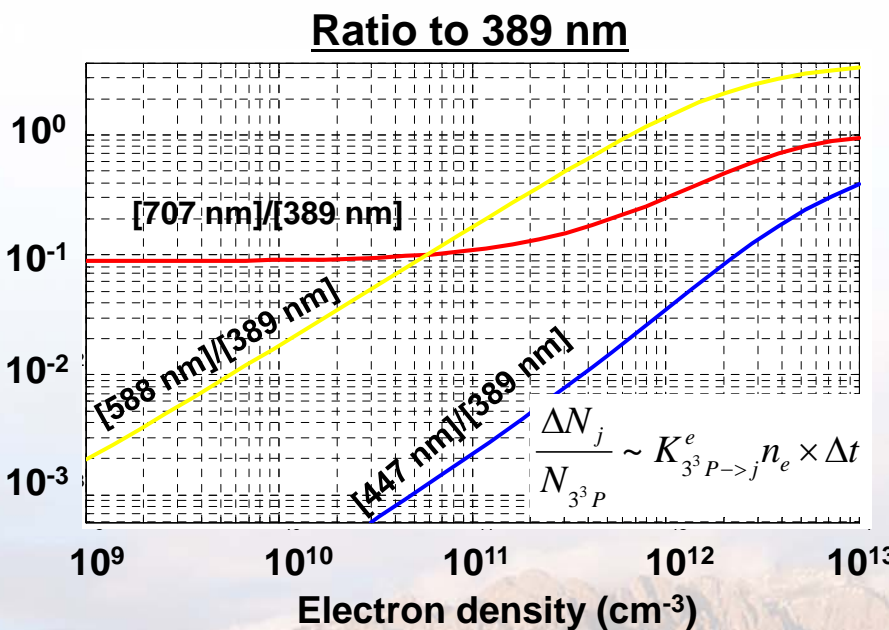
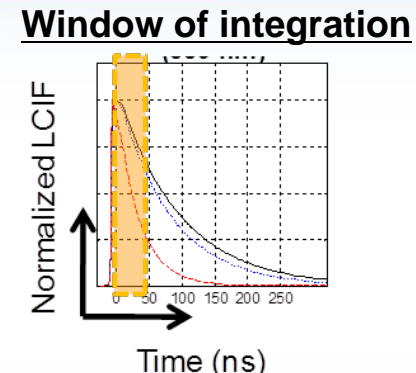


Sandia National Laboratories



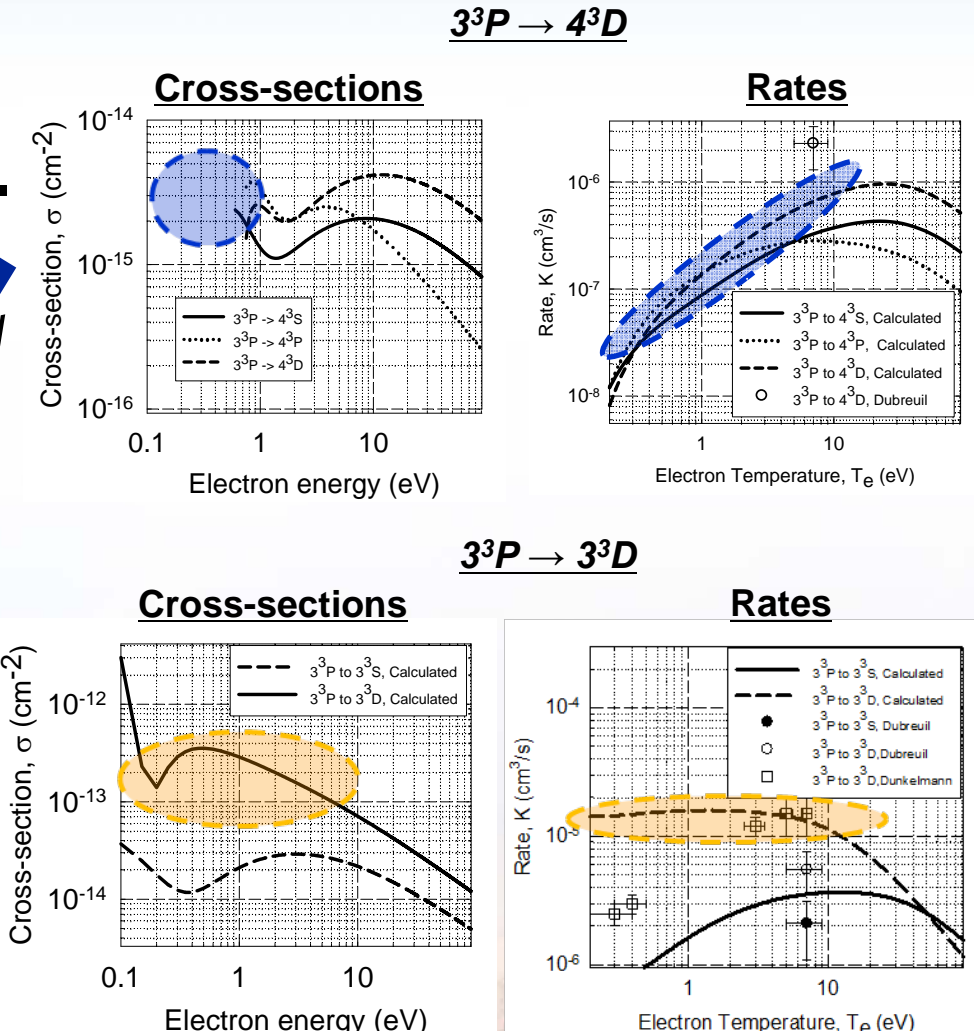
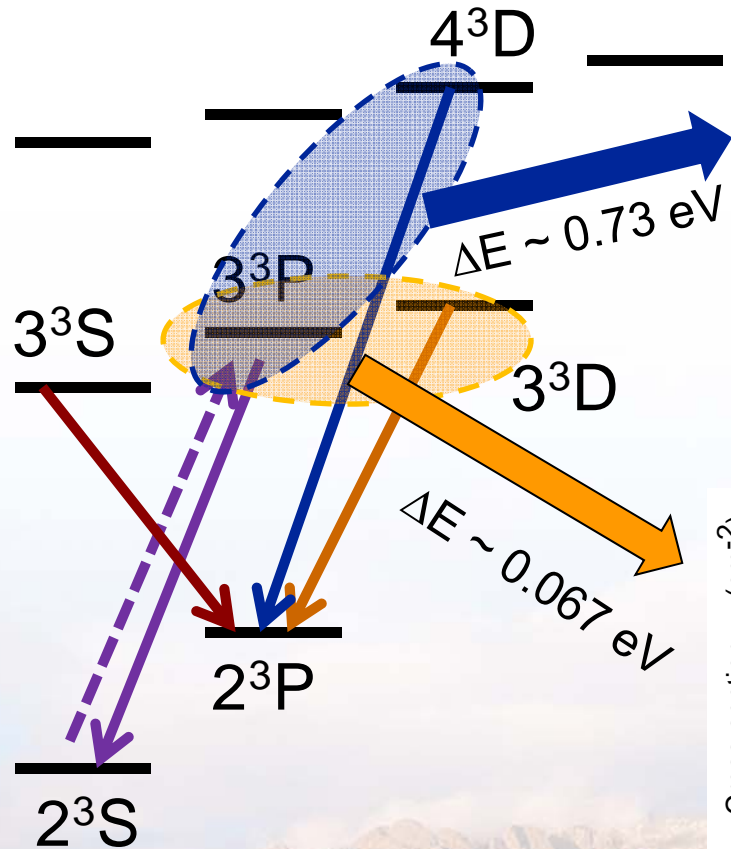
Time integrated intensity trends are utilized instead of time resolved LCIF

- Examine ratios of time integrated LCIF
 - Eliminates need for absolute calibrations
 - Still need relative efficiencies of imaging system
- Capitalize on "kT_e independent" coupling of 3³P to 3³D
 - Ratio of 588 nm to 389 nm yields n_e
 - Density + Ratio of 447nm to 588 nm yields kT_e



Only need to make three measurements to obtain n_e, kT_e

Small energy gap leads to "kT_e independent" coupling of 3³P to 3³D



Considerable fraction of the electrons are capable of driving the interaction

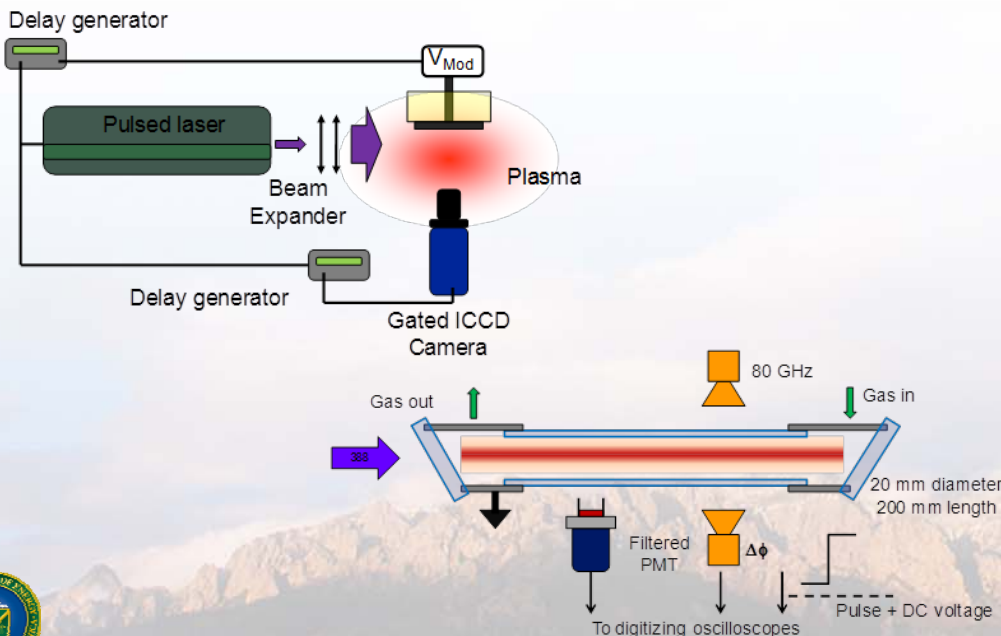


Part II: LCIF implementation and benchmark

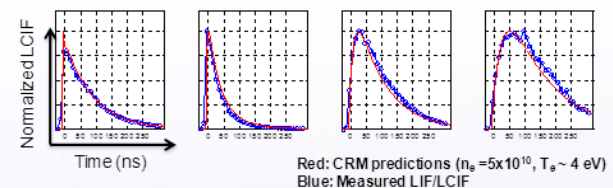
- **Implement and benchmark technique**

- Experimental considerations
- Benchmarking LCIF - compare observations with anticipated trends

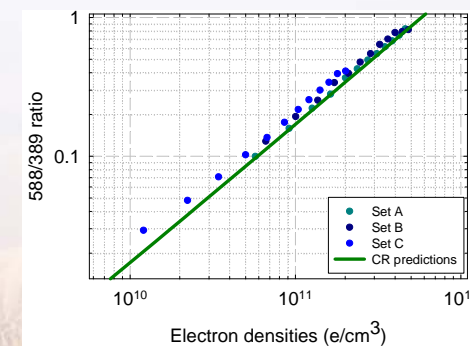
Experimental setup



Benchmark LCIF



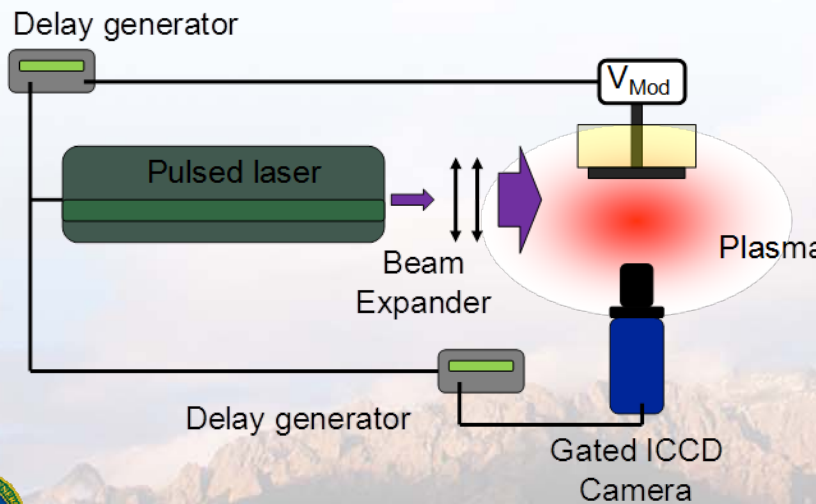
Red: CRM predictions ($n_e = 5 \times 10^{10}$, $T_e \sim 4$ eV)
Blue: Measured LIF/LCIF



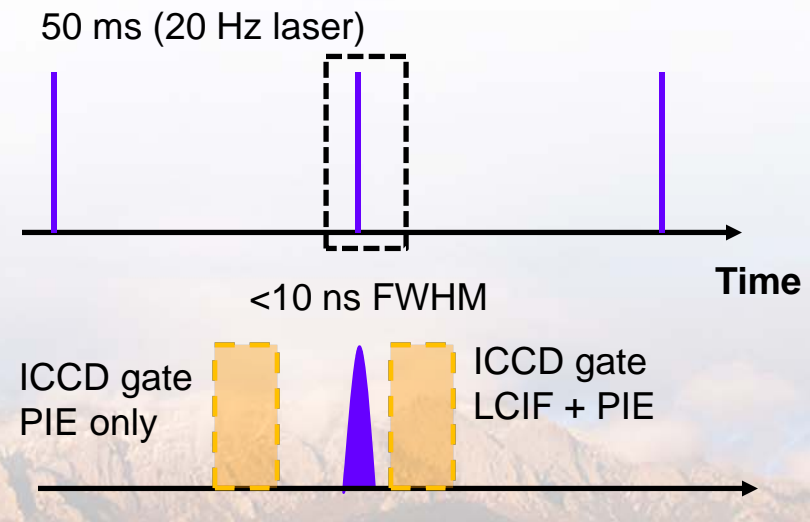
Experimental implementation of the LCIF is realized

- **Nanosecond pulsed laser used for excitation**
 - < 10 ns FWHM, < 0.1 cm⁻¹ line width
- **Timing of experiment controlled by delay generators**
 - Move experiment and imaging with respect to firing of the laser
- **Image LCIF with gated-intensified CCD**
 - Narrow (~ 1 nm FWHM) interference filters centered on lines of interest
- **Take two images per transition considered**
 - Total emission and plasma induced emission (PIE) - subtract the two

Optical setup



Timing sequence



Need to make six (3 x 2) measurements to obtain n_e , kT_e

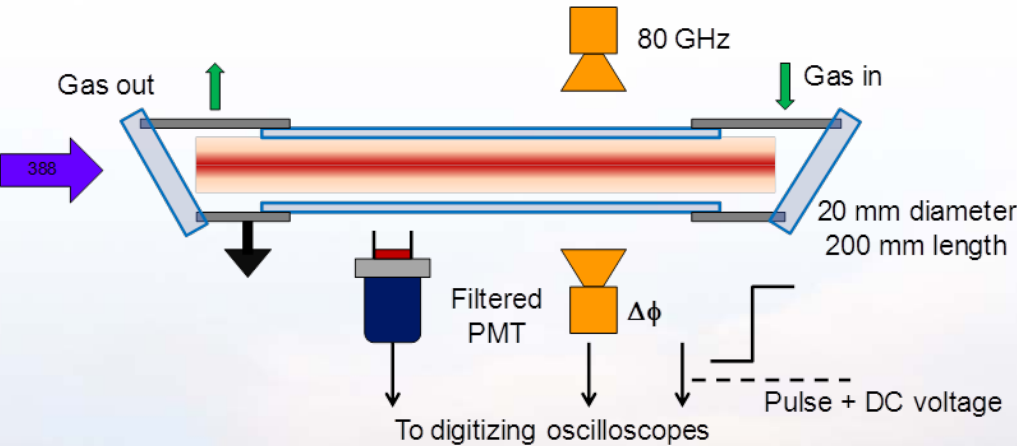


Sandia National Laboratories

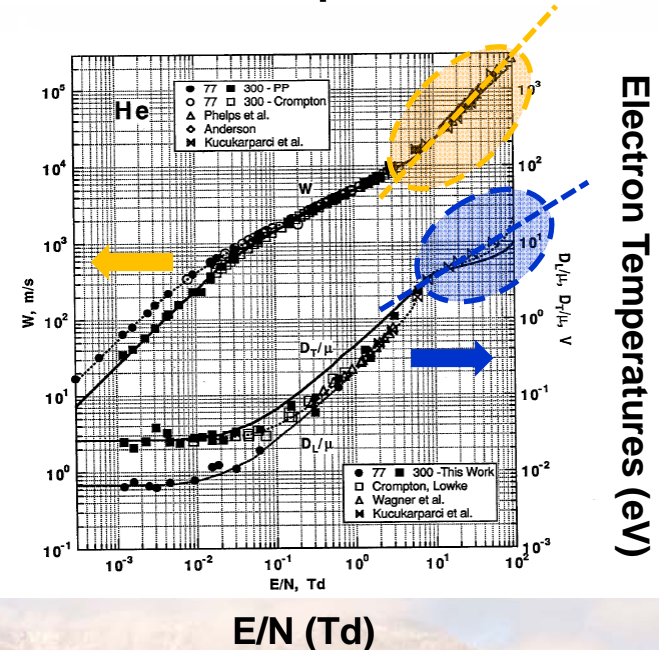
Pulsed positive column is utilized to benchmark LCIF technique

- Pulse discharge currents generate broad density range
 - ~ 10 Microseconds, 80 GHz interferometer
- Compute drift velocities and extract electron temperatures
 - Use published drift parameters

Positive column



Helium drift parameters



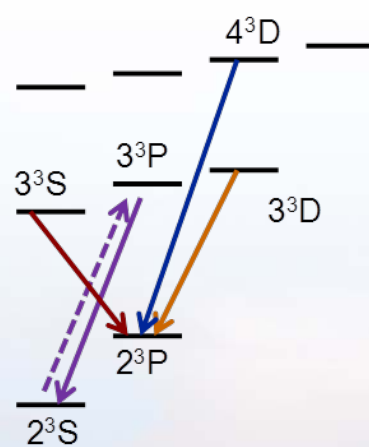
Positive column is a good vehicle to benchmark LCIF technique



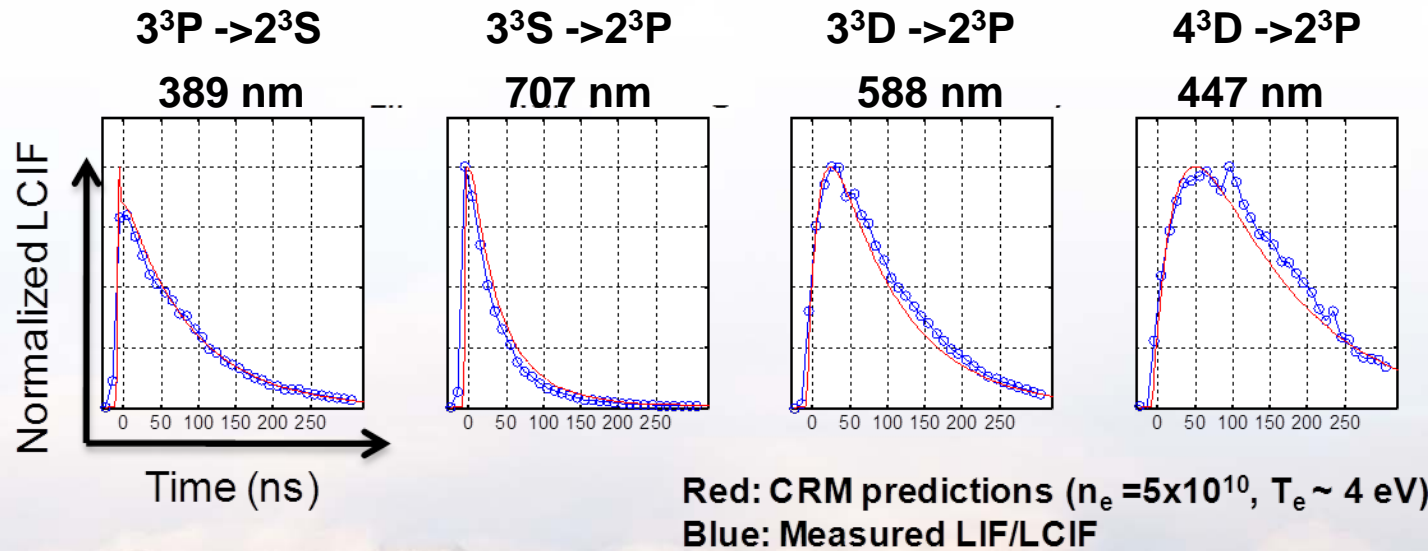
First steps: Verify time resolved LCIF to test CRM

- First sets of measurements presented some surprises
 - Strong radiative coupling between 3^3P and 3^3S states
- Proper accounting produced observed trends
 - Measured data and predicted behavior are consistent

Key transitions



Representative results

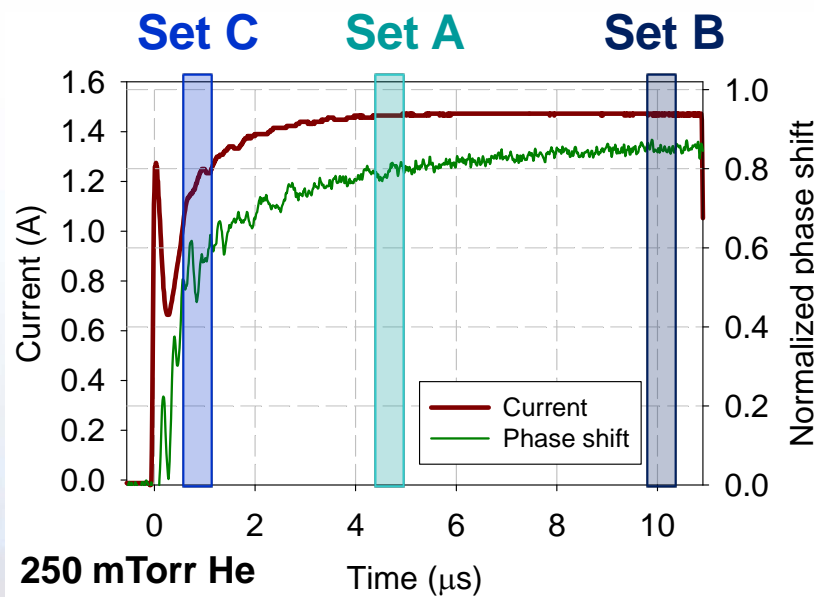


Good first demonstration of LCIF technique

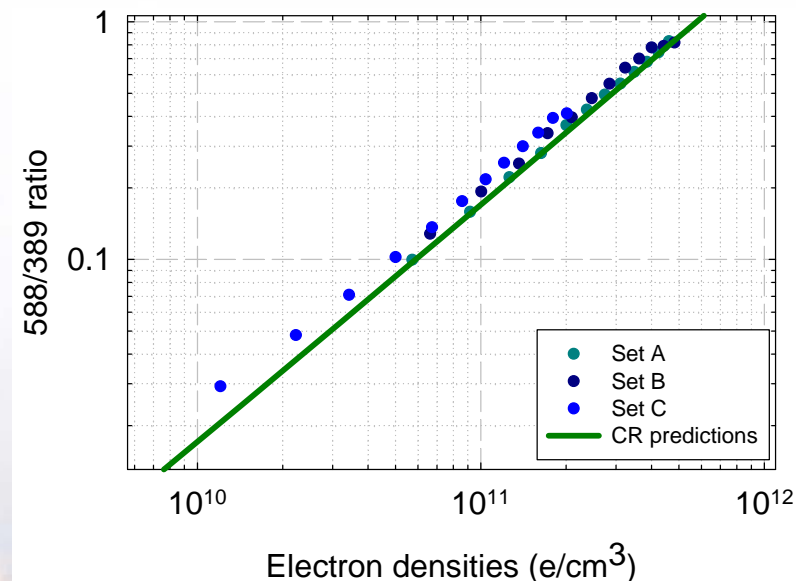
[588]/[389] ratio exhibits linearity over nearly two orders of magnitude

- Better yet, measured ratios agree reasonably well with computed ratios
 - Slightly higher, and some deviation at low density
- Examined trends at different times during the current pulse
 - Anticipate different temperatures as column is established

Waveforms during excitation



Density dependent ratio trends



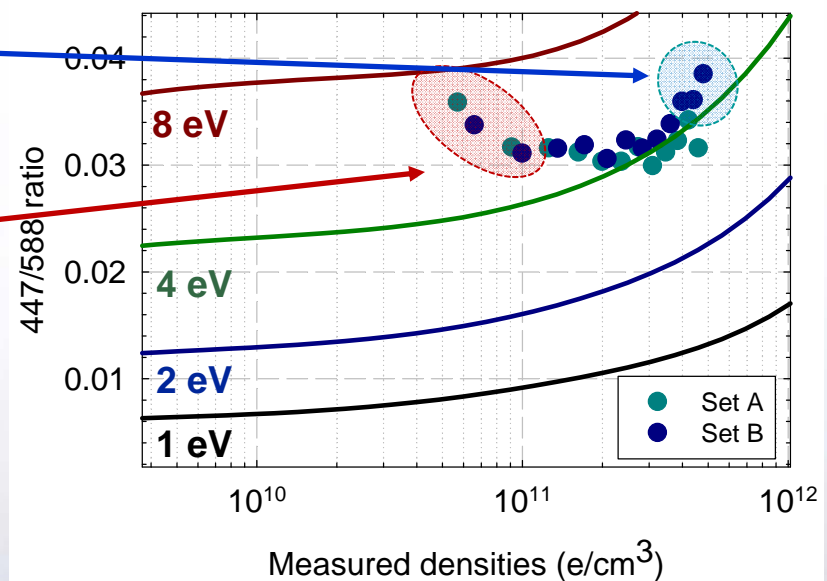
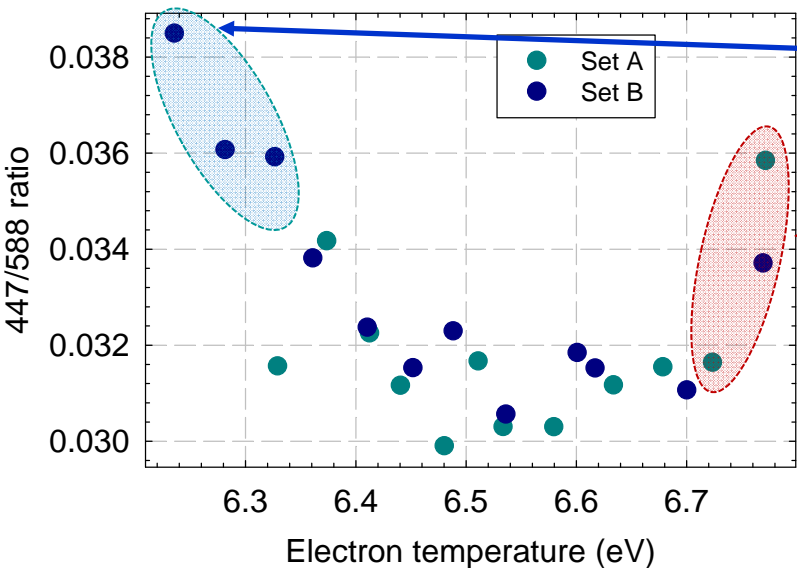
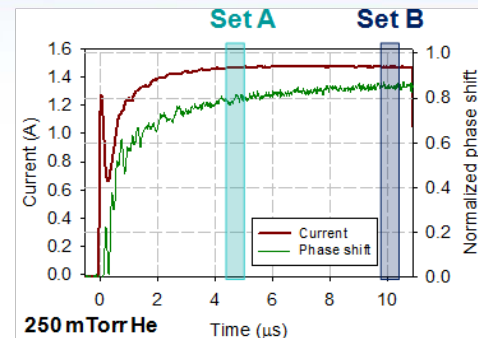
*Density measurements obtained at different times
essentially overlay each other*



Sandia National Laboratories

[447]/[588] ratio captures trends but misses absolutes

- Anticipated T_e trends are observed
 - High temperature at start, low temperatures later on
- Measure T_e trends mimic computed trends
 - Discrepancy in absolute values are apparent



Uncertainties in rates, EEDF and/or interpolation of T_e from drift parameters should impact absolute values

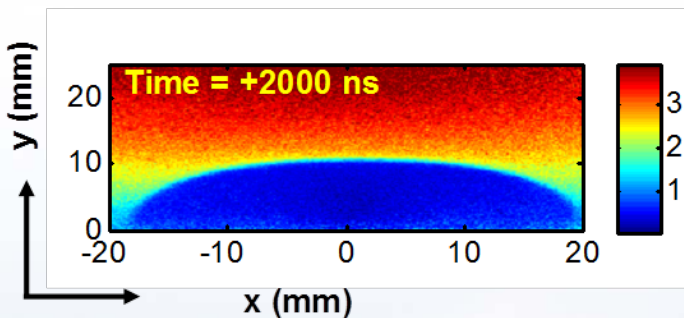


Sandia National Laboratories

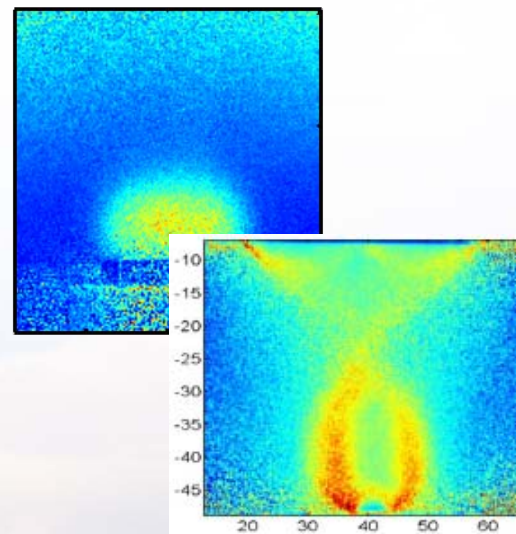
Part III: Applications of LCIF

- **Applications of LCIF**
 - ion sheaths, double layers and positive columns

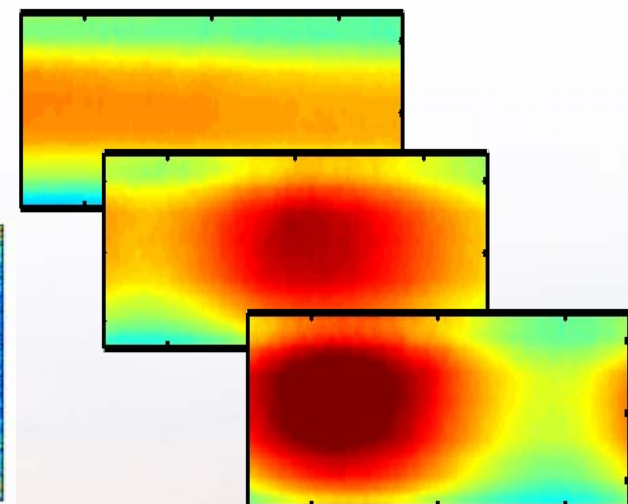
Ion sheath



Double layers



Striated positive column



Emphasize structure and evolution of the plasma being studied

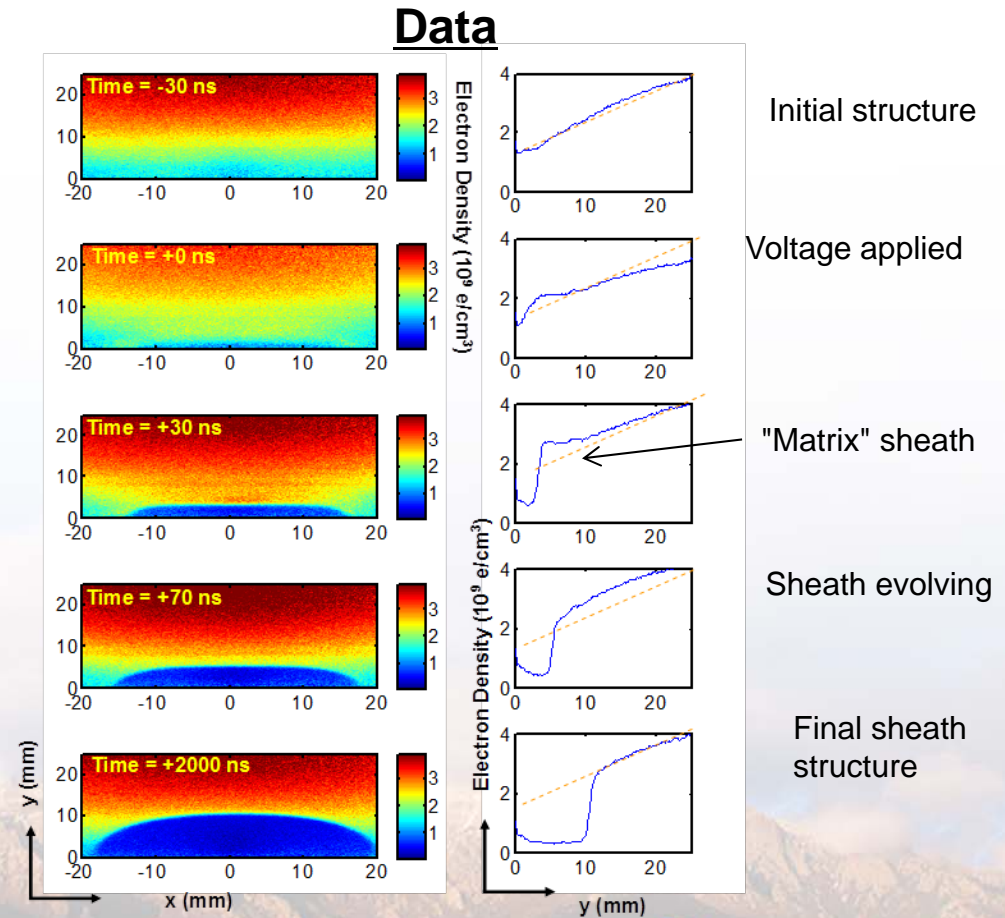
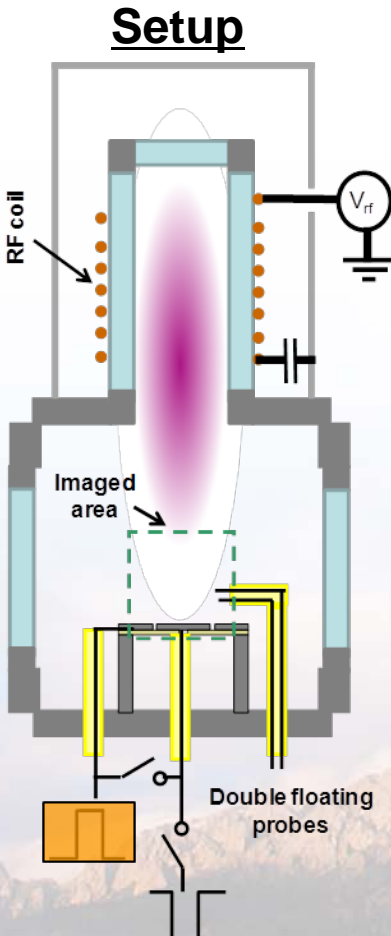


Sandia National Laboratories

Demonstration of LCIF technique: 2D-sheath formation

- Examine evolution and structure of ion sheath

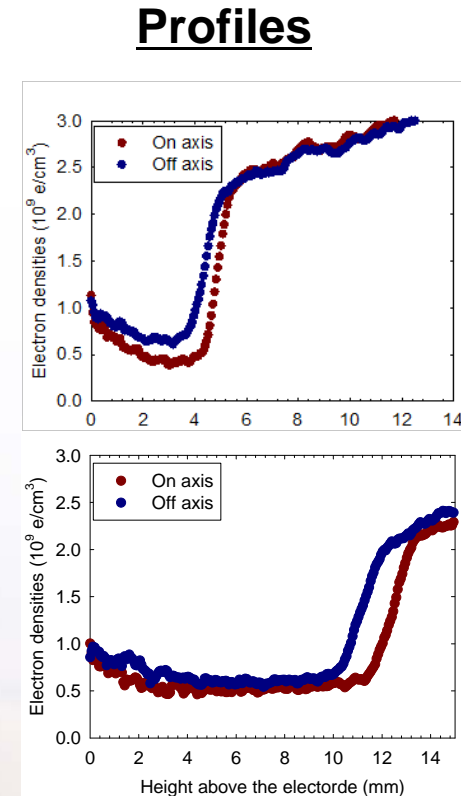
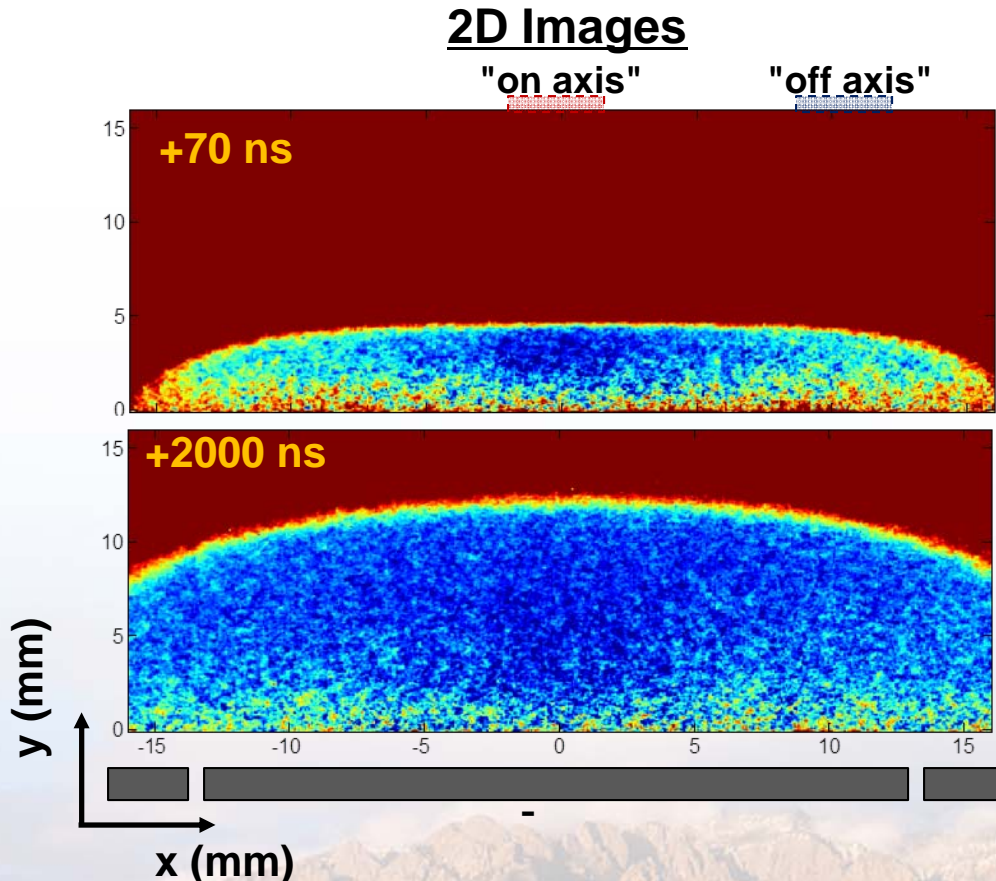
- 1 kV bias applied to inner electrode, 50 μ s into afterglow (low n_e , low kT_e)
- 20 ns snapshots of LCIF, 30 ns steps



Decent temporal and spatial resolution demonstrated

Interesting structure observed in the sheath

- LCIF signal observed deep in the sheath
 - Some caused by neutrals, but not all

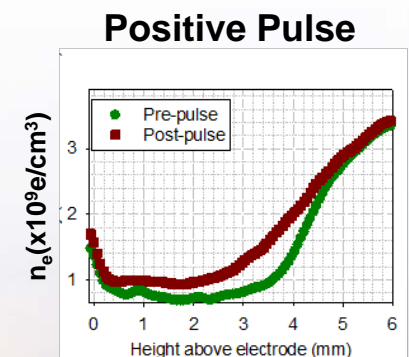
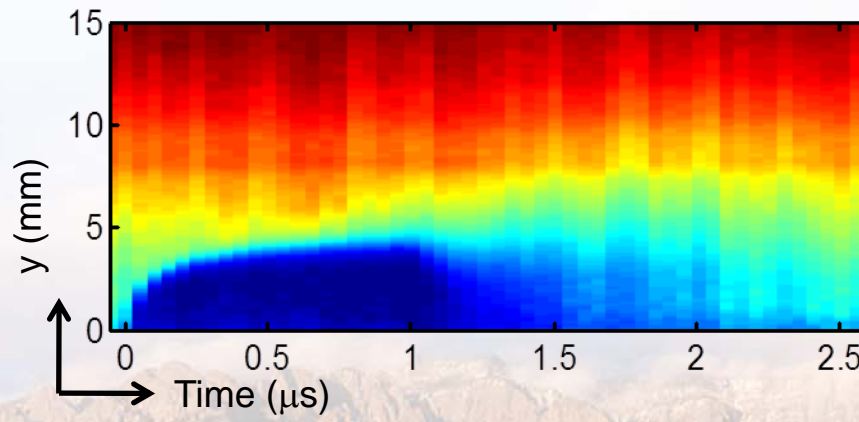
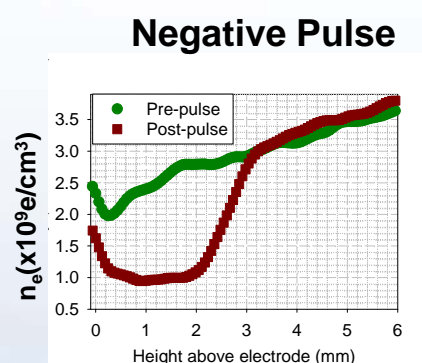
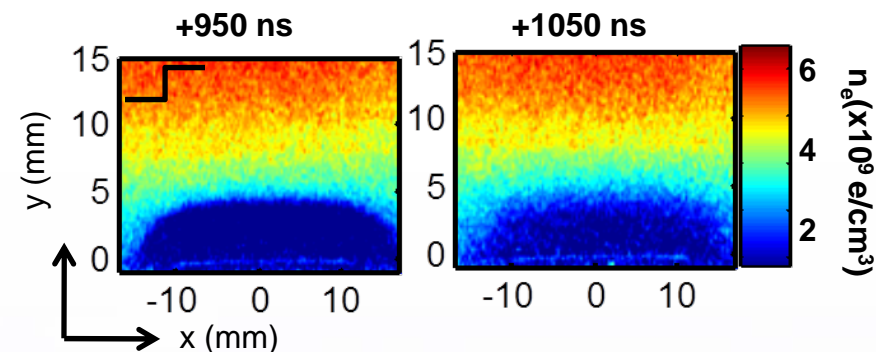
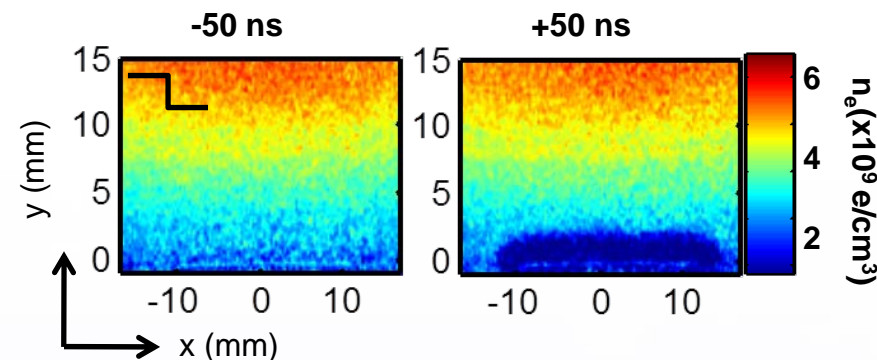
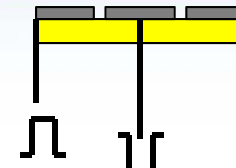


Signal deep in the sheath caused by electrons emitted from the electrode



Electrons backfill ion sheath after voltage is removed

- LCIF detects electrons but not ions
 - Examine time immediately after voltage is removed

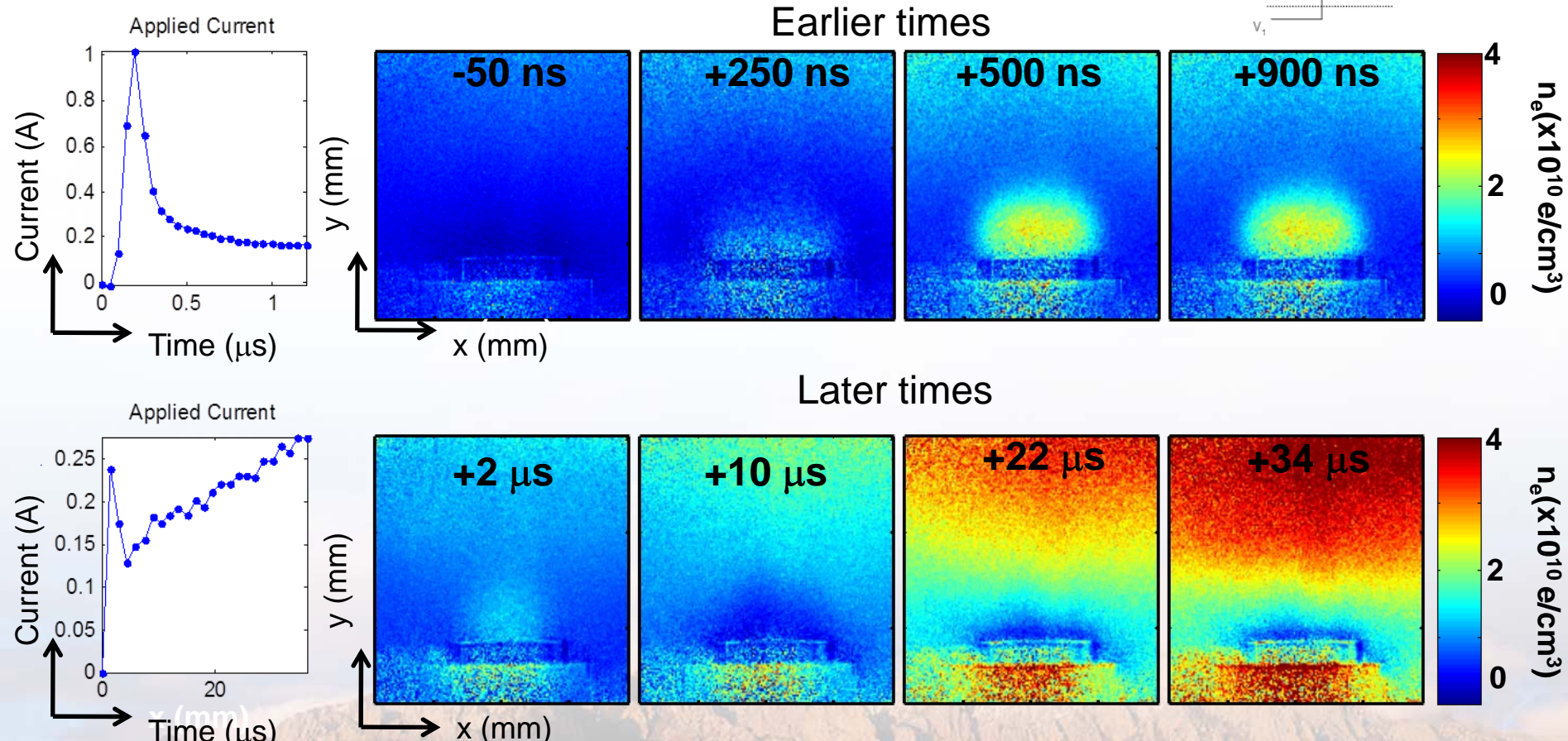
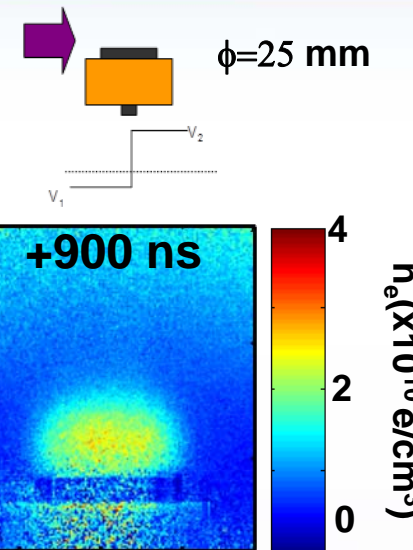




Transient anodic double layer observed after pulsed excitation

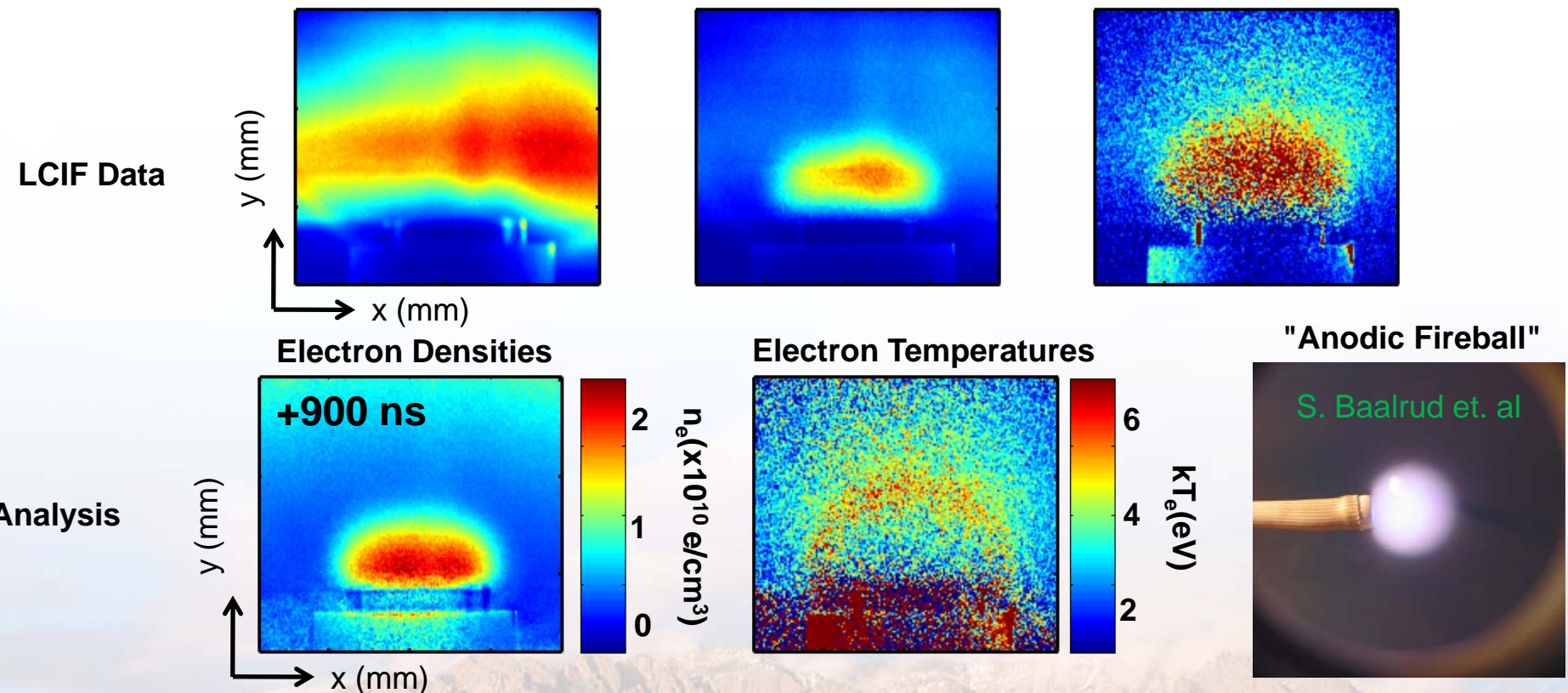
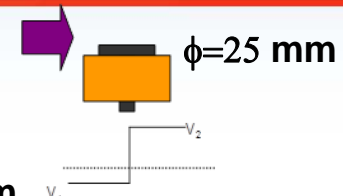
- Closer analysis of initial plasma distribution

- Use smaller (25 mm) diameter electrode, 100 mTorr afterglow



Higher energy electrons observed around edge of anode plasma

- Temperature measurements made for +900 ns case
 - Challenging measurement because of low level signals



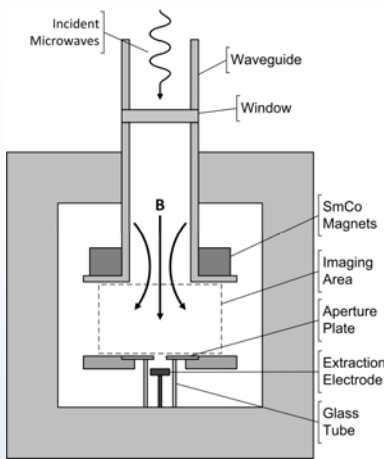
Electrons energized by localized electric fields supporting double layer



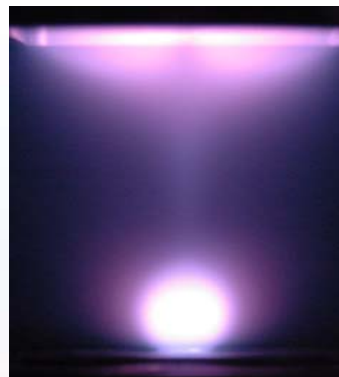
Double layer more pronounced in ECR based plasma cathodes

- NASA driven research interested in electron sources for propulsion
 - Understand limitations on current extraction
- Host Brandon Weatherford (U. Mich.) to implement LCIF
 - Examine coupling of between plasma generation and electron extraction

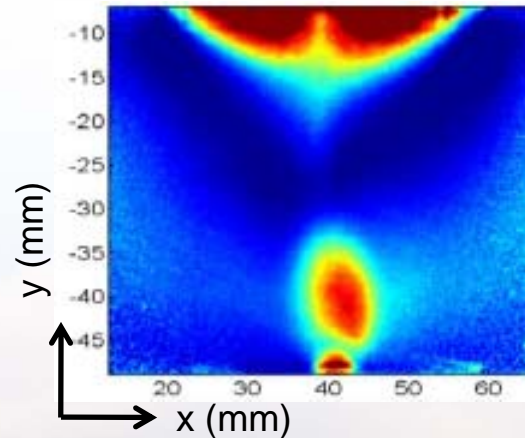
Setup



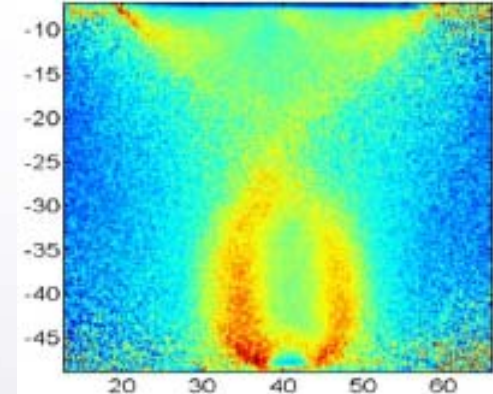
"Full color" picture



Density



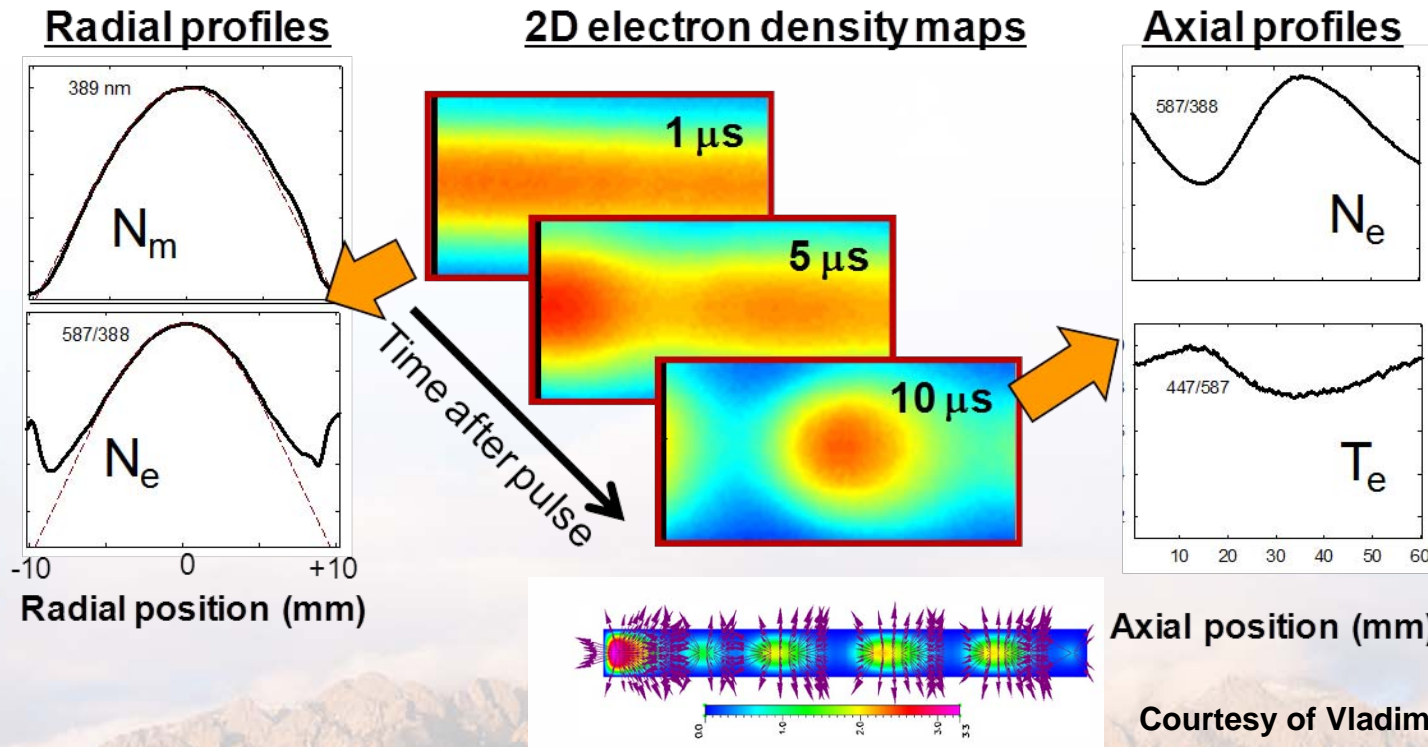
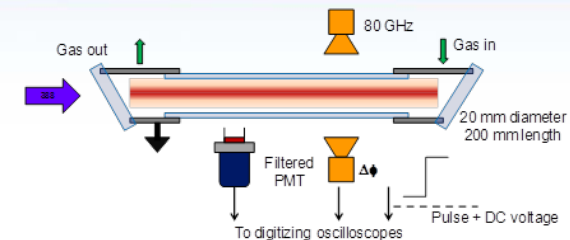
Temperature



*Multi-structure plasma formed by electron-extracting electrode...
... quite difficult to probe with more conventional means!*

LCIF is being used to study structure in a positive column

- Positive column is "well understood" system
 - Studied extensively, use it for calibration
- Platform for fast ionization wave (FIW) studies
 - Observations may warrant their own study



Courtesy of Vladimir Kolobov

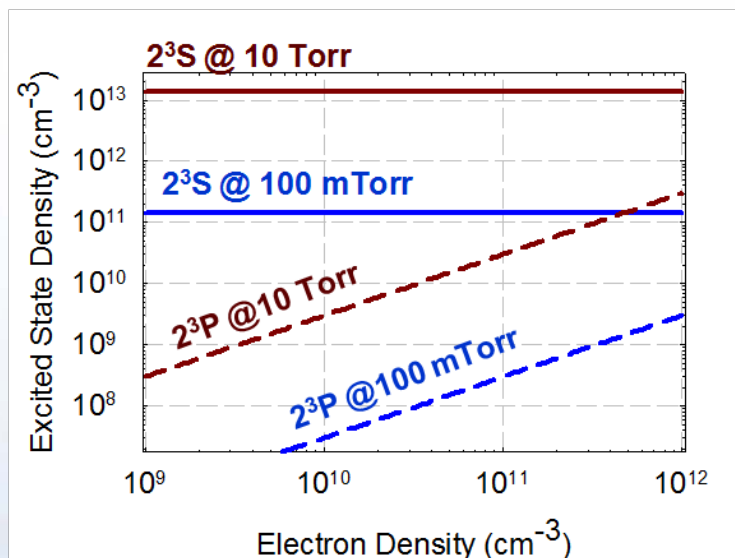
**Benchmark 2D simulations with measurements
made by LCIF**



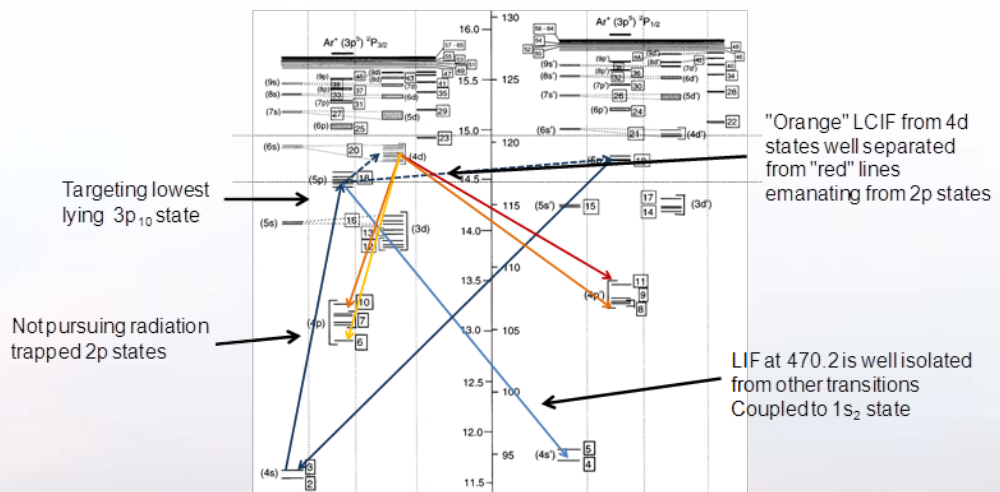
Part IV: Future pursuits with LCIF

- Extension of LCIF technique to other operating regimes
 - Limitations of helium and paths around this....

Extension of helium



Argon LCIF



Helium becomes limited at higher pressures

- Helium proved to be well suited for lower pressure and lower densities
 - Limited spectroscopic pathways
 - Well known cross-sections
 - Highly populated, long lived 2^3S metastable state
- As density increases and as composition changes
 - Radiation trapping/transport becomes problematic

$$\tau = L / l_{mfp} \approx f_{nm} \lambda \left(M c^2 / k T_A \right)^{1/2} N_A L \ll 1$$

Transition	f_{nm}	τ
$3^3P \rightarrow 2^3S$	0.064	>1
$4^3P \rightarrow 2^3S$	0.02	~1

(Assuming $L=1$ cm and $N_A \sim 10^{13}$ absorbers/cm³)

States connected to 2^3S can become trapped due to strong coupling and higher populations



Sandia National Laboratories

Pump out of alternative helium states

- At higher pressures and densities, 2^3P state becomes adequately populated
 - Comparable oscillator strengths (into comparable levels)
 - Sufficiently lower population compared to 2^3S

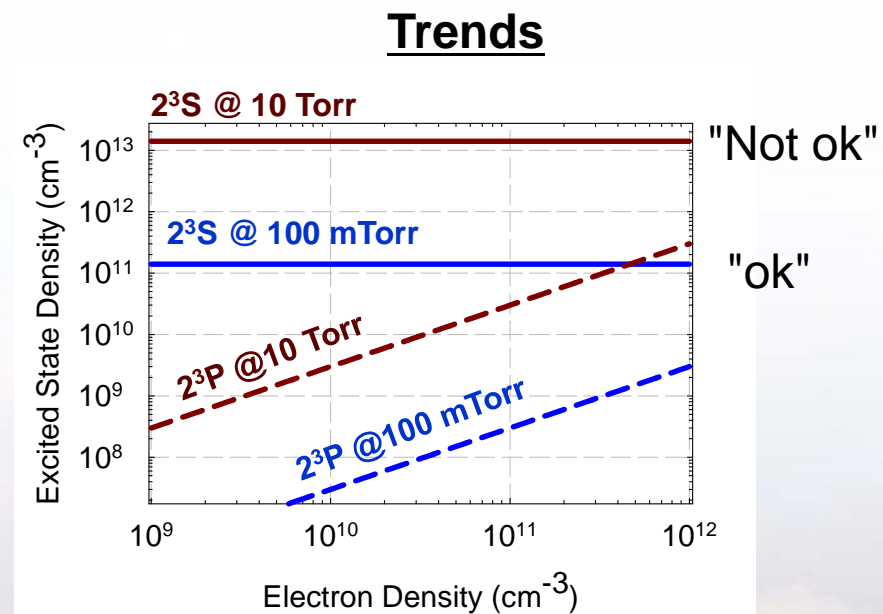
Scaling

2^3S State:

$$n_{2(3)S} \sim \frac{K_{0 \rightarrow S}^e}{K_{S \rightarrow P}^e} n_0 \sim 10^{-5} n_0$$

2^3P State:

$$n_{2(3)P} \sim \frac{1}{A_{P \rightarrow S}} [K_{0 \rightarrow P}^e + K_{S \rightarrow P}^e] n_0 n_e$$



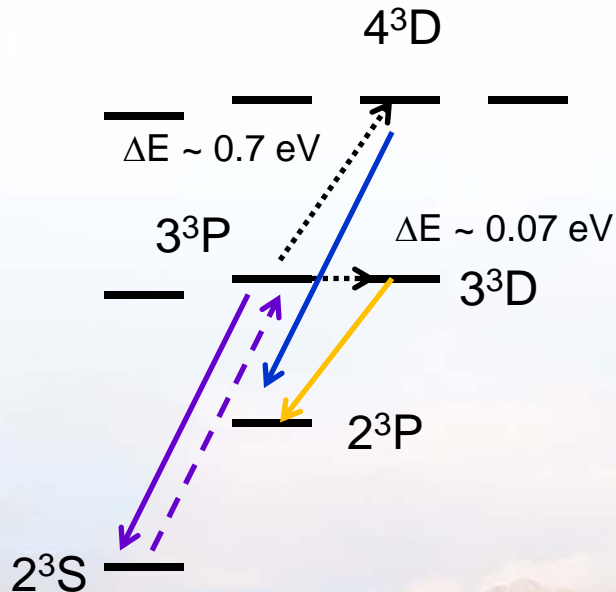
Low 2^3P state densities should be high enough to pump but low enough not to trap

Spectroscopic pathway proposed for pumping from 2^3P

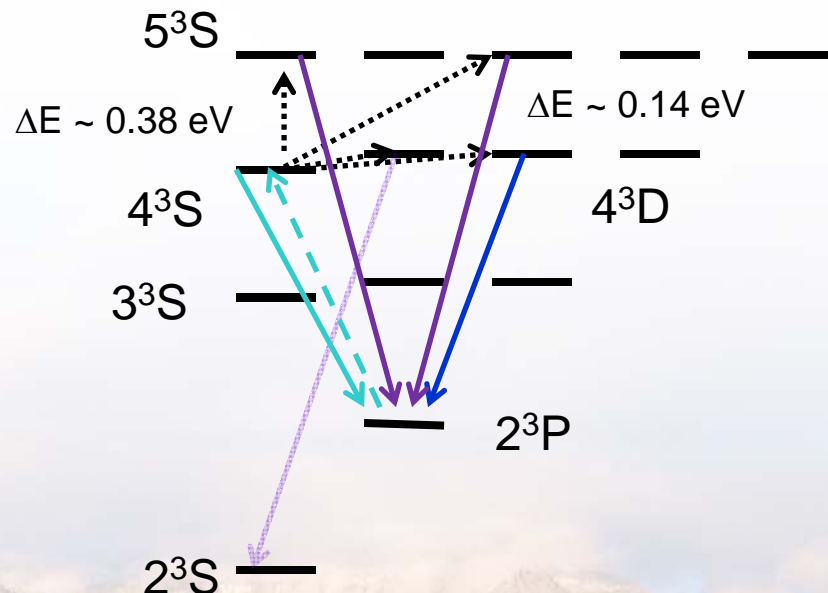
- Lower base density of 2^3P advantageous, but some tradeoffs

- Lose the nice "temperature free" $3^3P \rightarrow 3^3D$ transition
- Spectrally dense - many transitions ~ 400 nm

Previous approach



Proposed approach



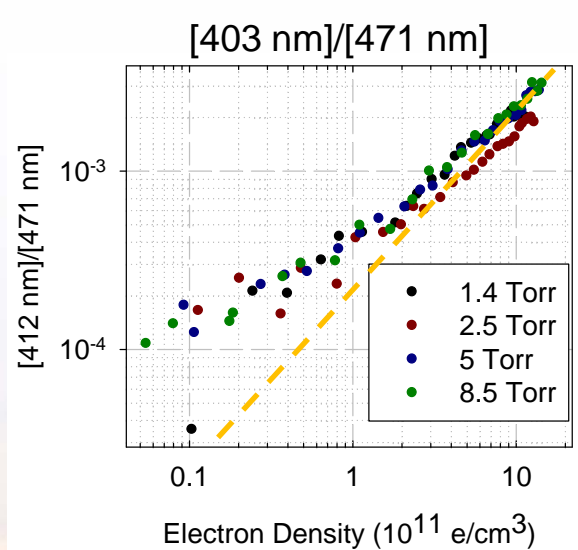
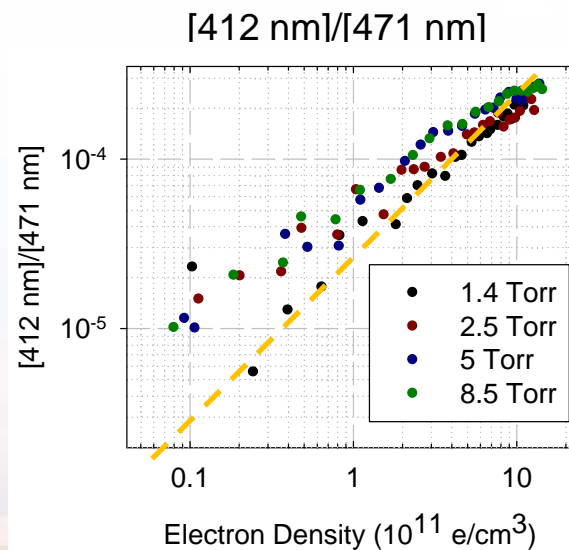
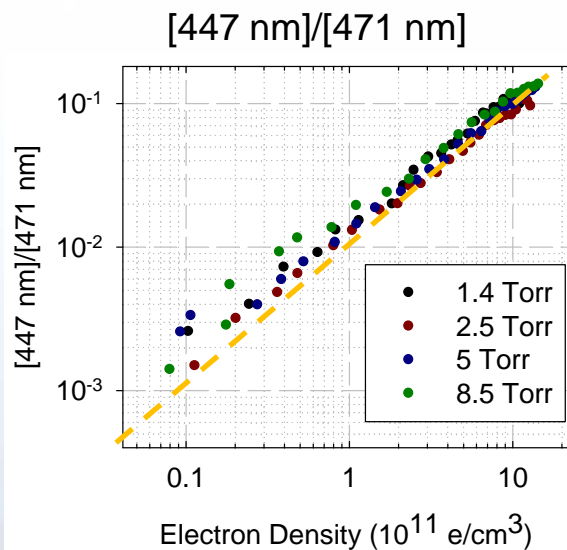
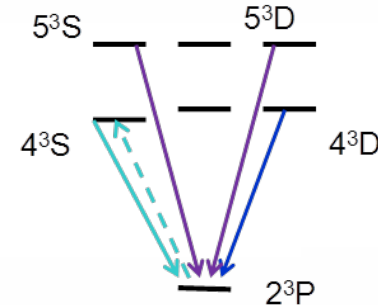
Pumping to the 3^3S or the 3^3D states are not "off the table" and may be pursued



Preliminary investigation of proposed scheme looks promising

- Employ same pulsed positive column used for 2^3S excitation

- Limit observations to states coupled to 2^3P
- Integration of 20 ns, 10 ns after laser excitation





Alternative gasses are being considered

- Technique is extendable to other gases
 - Helium is seldom "gas of choice"
 - Helium becomes problematic in mixtures
- Argon is commonly used gas and obvious choice
 - More pump-probe pathways to consider
 - Individual lower lying $1s_x$ states are anticipated to less populated

$$\tau = L / l_{mfp} \approx f_{nm} \lambda \left(M c^2 / k T_A \right)^{1/2} N_A L \ll 1$$

Helium

Transition	f_{nm}	τ
$3^3P \rightarrow 2^3S$	0.064	>1
$4^3P \rightarrow 2^3S$	0.02	~1

Argon

Transition	f_{nm}	τ
$2p_{10} \rightarrow 1s_5$	0.17	>>1
$3p_{10} \rightarrow 1s_5$	9×10^{-4}	0.08

(Assuming $L=1$ cm and $N_A \sim 10^{13}$ absorbers/cm³)



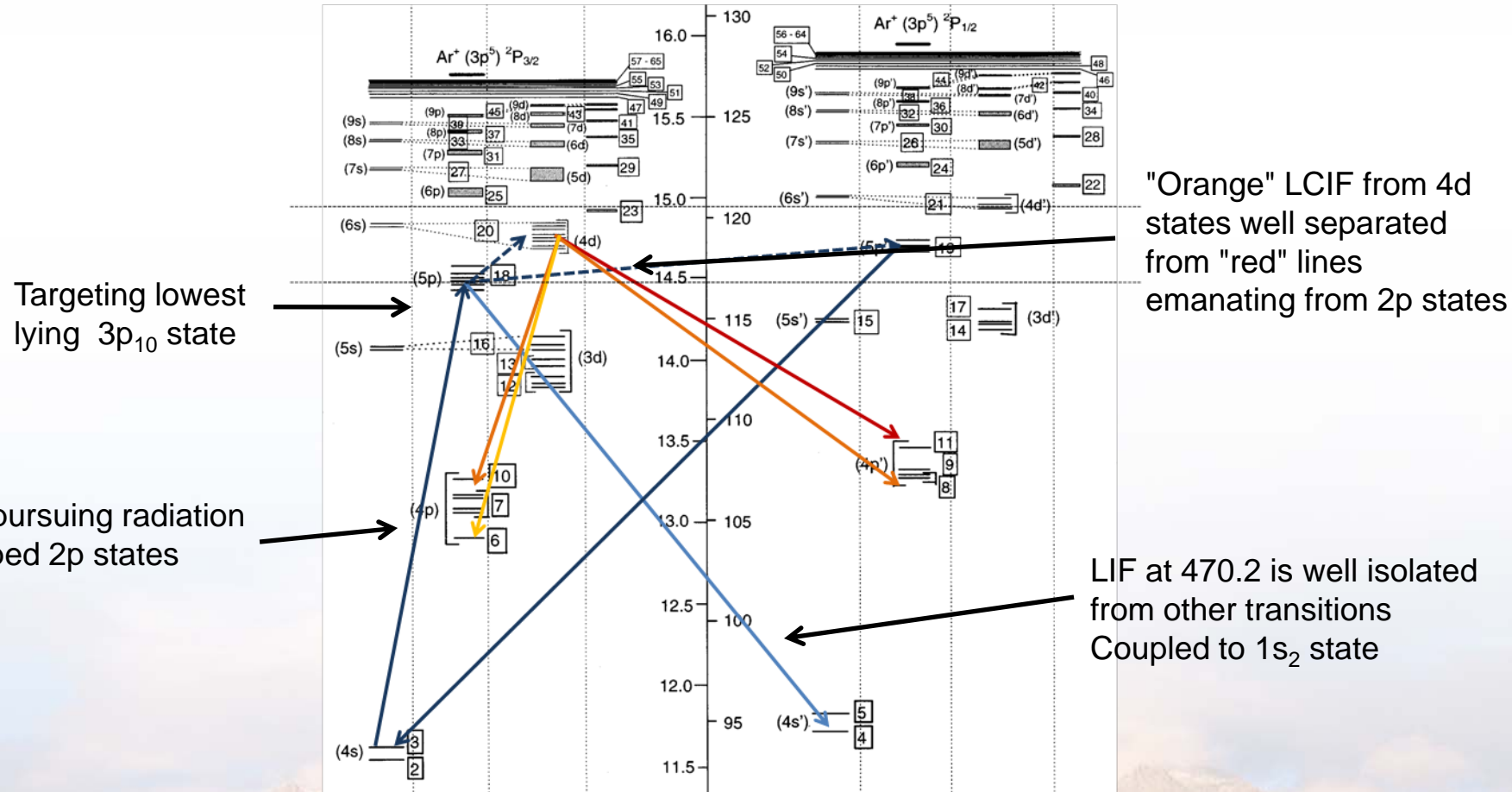
Low oscillator strengths and possibly lower densities make argon attractive



Sandia National Laboratories

Complexity of argon makes extension of LCIF "challenging"

- Argon offers more spectroscopic pathways to pursue



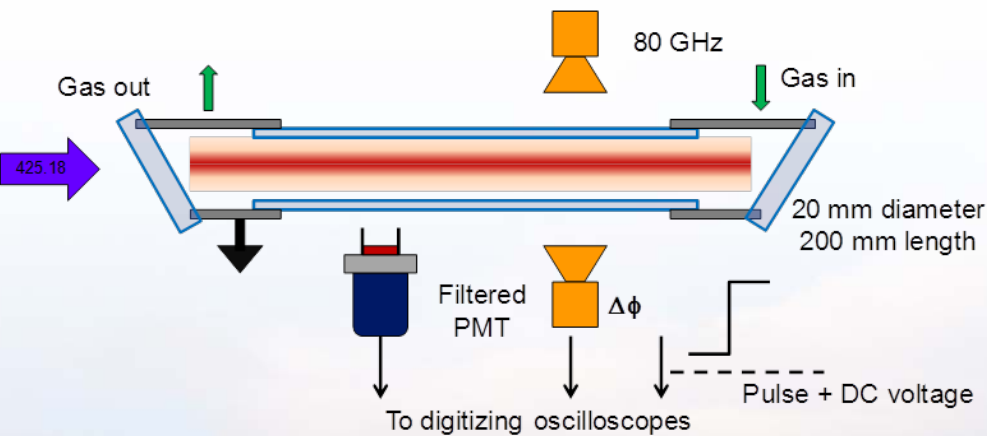
Taken from Bogearts et. al, J. Appl. Phys. **84**, 121, 1998

Cross sections and rates not well known for electronic driven processes from 3p to higher states

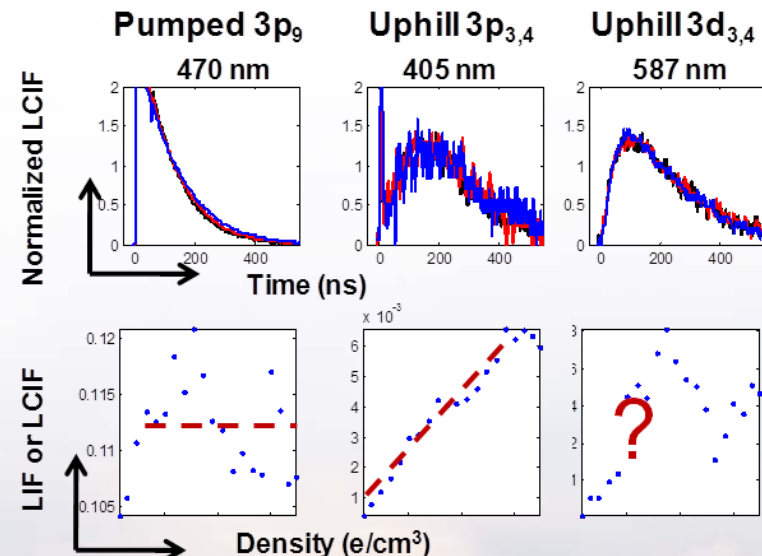
Despite reservations Argon LCIF is being investigated

- Well characterized positive column is used to test feasibility
 - Microwave interferometer to measure densities
 - Pulsed for higher densities/temperatures and stable plasmas
 - Time resolved LIF/LCIF with PMT + narrowband filters

Calibration cell



Preliminary trends



Perspective transitions are identified and calibration of the technique is underway Stay tuned!





Concluding remarks and future directions

- **LCIF technique demonstrated in 2D**
 - Free of “line of sight” constraints
 - Good spatial resolution – limited by optical collection
 - Decent temporal resolution – limited by ICCD gate times & tolerable signals
- **Caution required for proper implementation of the technique**
 - Uncertainties about rates – Absolute bounds on measurements
 - Proper choice of model – Capture the required physics
- **Technique should be extendable over broad parameter space**
 - Higher pressures – neutral collisions
 - Smaller dimensions – scattering and access
 - Other atomic systems

*This work was supported by the Department of Energy Office of Fusion Energy Science
Contract DE-SC0001939*



Sandia National Laboratories



Thank you



Sandia National Laboratories

Neutral mixing of 3^3P and 3^3D needs to be considered

- Proximity (energetically) of states means neutrals can transfer excited population to 3^3D
 - Energy spacing between states is 0.067 eV \sim 780 K

Amount of 3^3D produced from 3^3P

$$\Delta N_{Electrons} \sim K_{P \rightarrow D}^e n_e \Delta N_P \Delta t \quad \text{and}$$

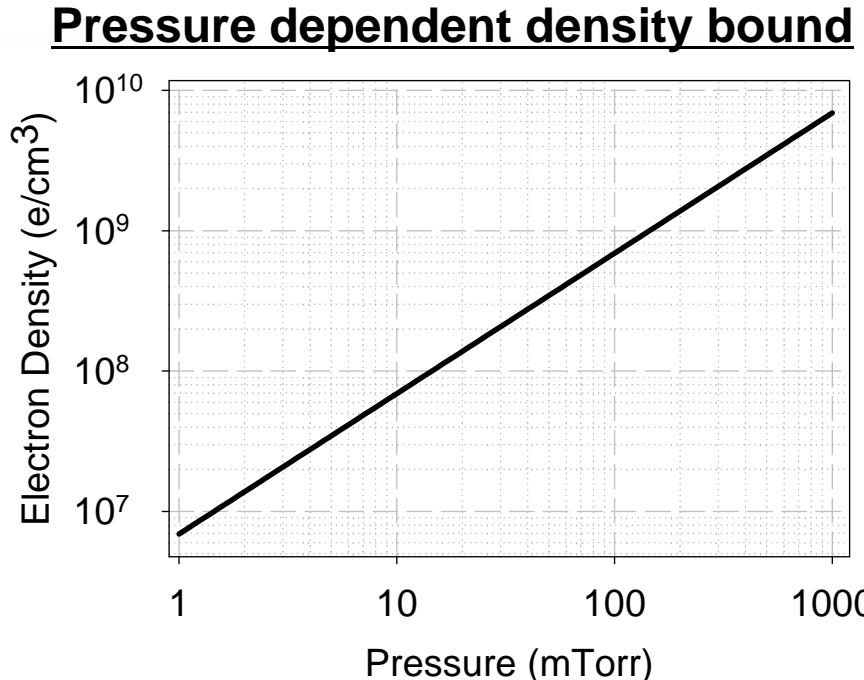
$$\Delta N_{Neutrals} \sim K_{P \rightarrow D}^N n_0 \Delta N_P \Delta t$$

Bound determined by setting the two equal

$$\frac{\Delta N_{Electrons}}{\Delta N_{Neutrals}} \sim \frac{K_{P \rightarrow D}^e n_e}{K_{P \rightarrow D}^N n_0} \sim 1$$

Solve for n_e

$$n_e \sim \frac{K_{P \rightarrow D}^N}{K_{P \rightarrow D}^e} n_0 \sim \frac{10^{-12}}{10^{-5}} n_0$$



Lower limit on electron density scales with pressure (and temperature) of neutral background





References for rates and cross-sections

■ Superelastic

- Klein Rosseland
- Sobelman

$$K_{ij}^e = \left\langle \sigma_{ij} v_e \right\rangle = \left(\frac{m_e}{2\pi k T_e} \right)^{1/2} \int_0^{\infty} \sigma_{ij}(v) \exp\left(\frac{-m_e v^2}{2k_B T_e}\right) 4\pi v^2 dv \left[\frac{g_j}{g_i} \exp\left(\frac{(E_j - E_i)}{k_B T_e}\right) \right]$$

[1] C. F. Burrell and H.-J. Kunze, Phys. Rev. A **18**, 2081 (1978).

[1] P. Chall, E. K. Souw and J. Uhlenbusch, J. Quant. Spectrosc. Radiant. Transfer **34**, 309 (1985).

[1] G. Dilecce, P. F. Ambrico and S. De Benedictis, J. Phys. B: At. Mol. Opt. Phys. **28**, 209 (1994).

[1] R. Denkelmann, S. Maurmann, T. Lokajczyk, P. Drepper, and H. -J. Kunze, J. Phys. B: At. Mol. Opt. Phys. **32**, 4635 (1999).

[1] R. Denkelmann, S. Freund and S. Maurmann, Contrib. Plasma Phys. **40**, 91 (2000).

[1] K. Tsuchida, S. Miyake, K. Kadota and J. Fujita, Plasma Physics **25**, 991 (1983).

[1] B. Dubreuil and P. Prigent, J. Phys. B: At. Mol. Opt. Phys. **18**, 4597 (1985).

[1] E. A. Den Hartog, T. R. O'Brian and J. E. Lawler, Phys. Rev. Lett. **62**, 1500 (1989).

[1] K. Dzierzega, K. Musiol, E. C. Benck and J. R. Roberts, J. Appl. Phys. **80**, 3196 (1996).

[1] L. Maleki, B. J. Blasenheim, and G. R. Janik, J. Appl. Phys. **68**, 2661 (1990).

[1] R. S. Stewart, D. J. Smith, I. S. Borthwick and A. M. Paterson, Phys. Rev. E **62**, 2678 (2000).

[1] R. S. Stewart, D. J. Smith, J. Phys. D: Appl. Phys. **35**, 1777 (2002).

[1] A. Hidalgo, F. L Tabares and D. Tafalla, Plasma Phys. Control. Fusion **48**, 527 (2006).

[1] D. A. Shcheglov, S. I. Vetrov, I. V. Moskalenko, A. A. Skovoroda and D. A. Shubaev, Plasma Phys. Rep. **32**, 119 (2006).

[1] M. Krychowiak, Ph Mertens, R. Konig, B. Schweer, S. Brezinsek, O. Schmitz, M. Brix, U. Samm and T. Klinger, Plasma Phys. Control. Fusion **50**, 65015 (2008).

[1] K. Takiyama, H. Sakai, M. Yamasaki, and T. Oda, Jpn. J. Appl. Phys. **33**, 5038 (1994).

[1] M. Watanabe, K. Takiyama, H. Toyota Jpn. J. Appl. Phys. **38**, 4380 (1999).

[1] G. Nersisyan, T. Morrow, and W. G. Graham, Appl. Phys. Lett. **85**, 1487 (2004).

[1] W. L Wiese, M. W. Smith, and B. M. Glennon, *Atomic Transition Probabilities 4/V1* (Nat. Stand. Ref. Data. Ser., Nat. Bur. Stand. Washington DC, 1966).

[1] Yu. Ralchenko, R. K. Janev, T. Kato, D. V. Fursa, I. Bray, F. J. De Heer, Atomic Data and Nuclear Data Tables **94**, 603 (2008).

[1] I.I. Sobelman, L. A. Vainshtein, and E. A. Yukov, *Excitation of Atoms and Broadening of Spectral Lines* (Springer, New York, 1981) p. 5.

$$K_{ij}^e = \left\langle \sigma_{ij} v_e \right\rangle = \left(\frac{m_e}{2\pi k T_e} \right)^{1/2} \int_0^{\infty} \sigma_{ij}(v) \exp\left(\frac{-m_e v^2}{2k_B T_e}\right) 4\pi v^2 dv$$





Further experiments point to where improvement is needed

- Here is the "ugly" data
 - Predicted trends approach measured trends
- Two data sets offer some clues
 - Low pump power and low concentration of species
- Stimulated emission inducing 3^3P to 3^3S transition?
 - Population inversion: $N_P \gg N_S$ after excitation

$$\frac{dN_S}{dt} = AN_P + A\left(\frac{\lambda^2}{8\pi}\right)g(\nu)\left(N_P - \frac{g_2}{g_1}N_S\right)\frac{I}{h\nu}$$

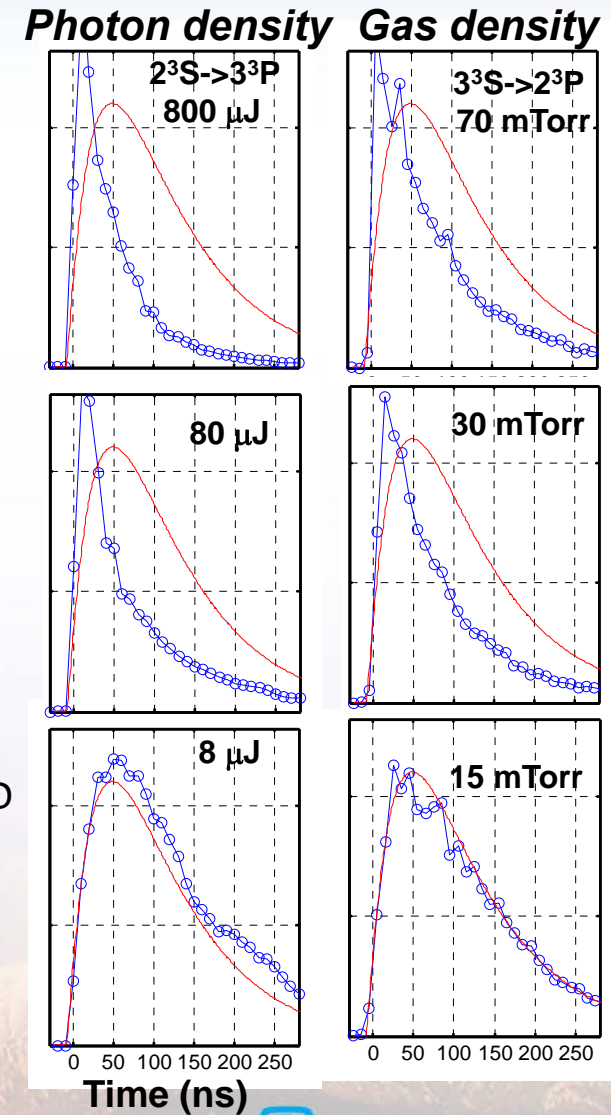
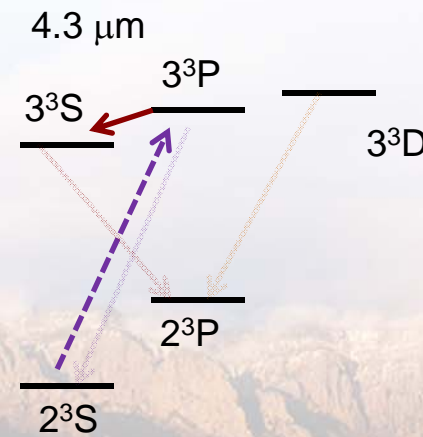
Spontaneous Emission
Stimulated emission & absorption

After pumping inversion occurs

$$\frac{dN_S}{dt} \approx A_{eff}N_P, \quad N_P \gg N_S$$

Where

$$A_{eff} = A\left[1 + \left(\frac{\lambda^2}{8\pi}\right)g(\nu)\frac{I}{h\nu}\right] > 10^8 s^{-1}?$$



More complete treatment should include photon densities





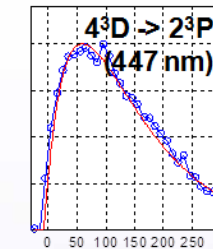
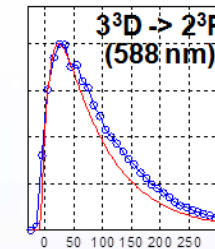
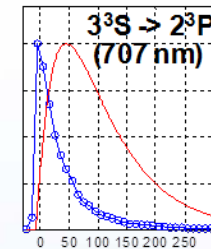
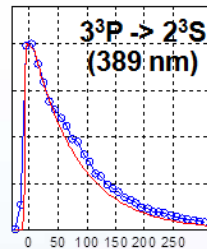
Complete treatment bypassed through simplifying approximations

- Assume population inversion occurs only during laser excitation
 - Side step need to track absolute photon intensities

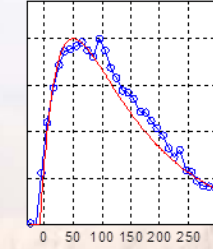
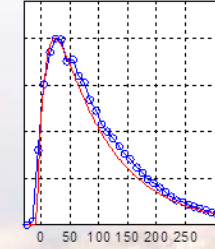
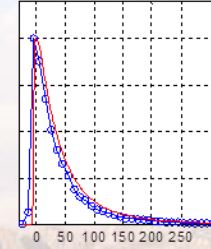
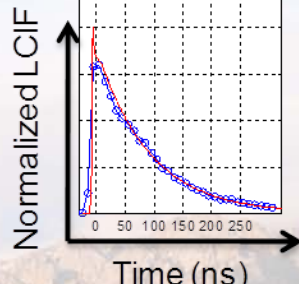
$$A_{Eff} = A_{Nom} \left[1 + A_{Inv} e^{-\frac{I_{Laser}}{I_{Threshold}}} \right]$$

Normalized time resolved trends

Data Set A: $A_{Eff} = A_{Nom}$



Data Set B: $A_{Eff} \gg A_{Nom}$ (During laser excitation)



Red: CRM predictions ($n_e = 5 \times 10^{10}$, $T_e \sim 4$ eV)
Blue: Measured LIF/LCIF

Simplifying assumption produces trends consistent with observation

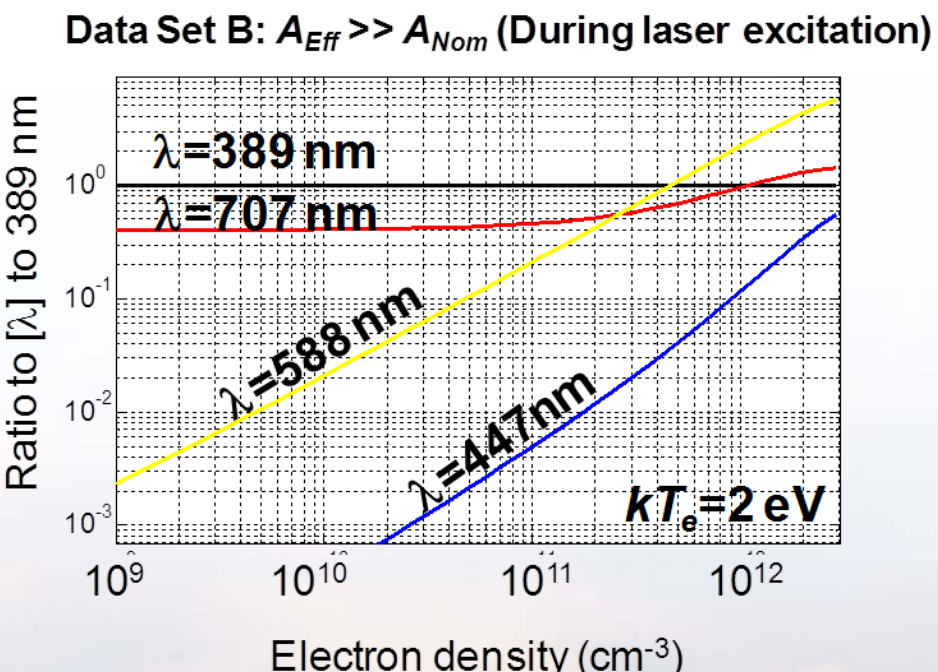
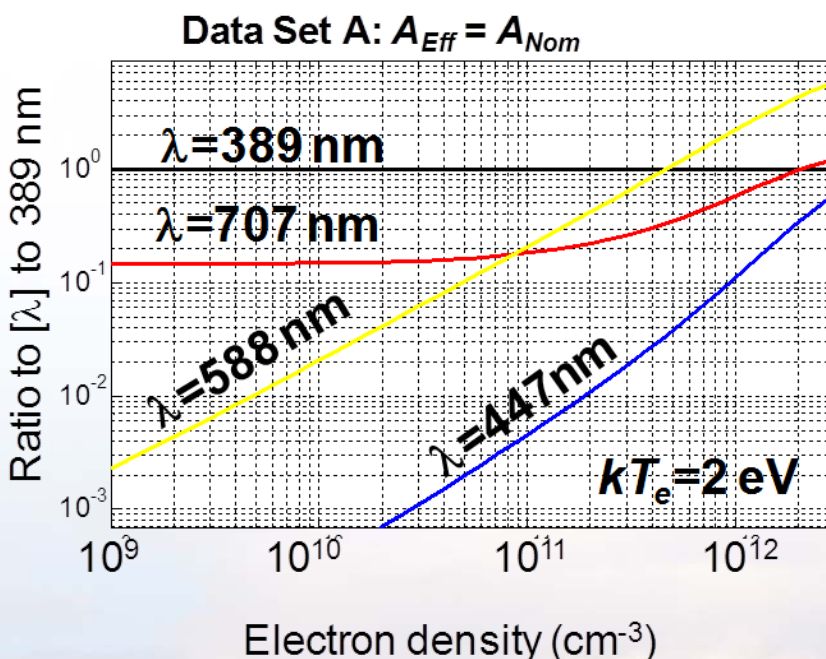


Sandia National Laboratories

Key uphill transitions are not significantly impacted by radioactive coupling

- Dominant population pathway is still through excited 3^3P state
 - Final densities of 3^3P state will change, but this is normalized out in analysis

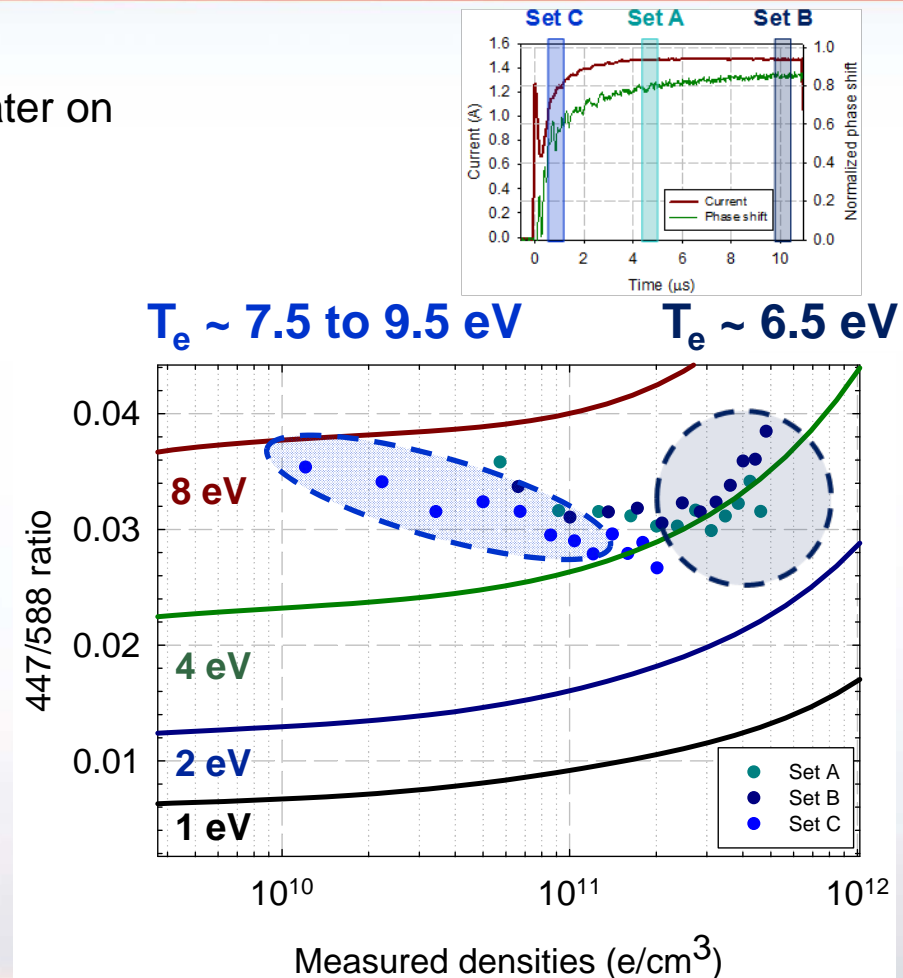
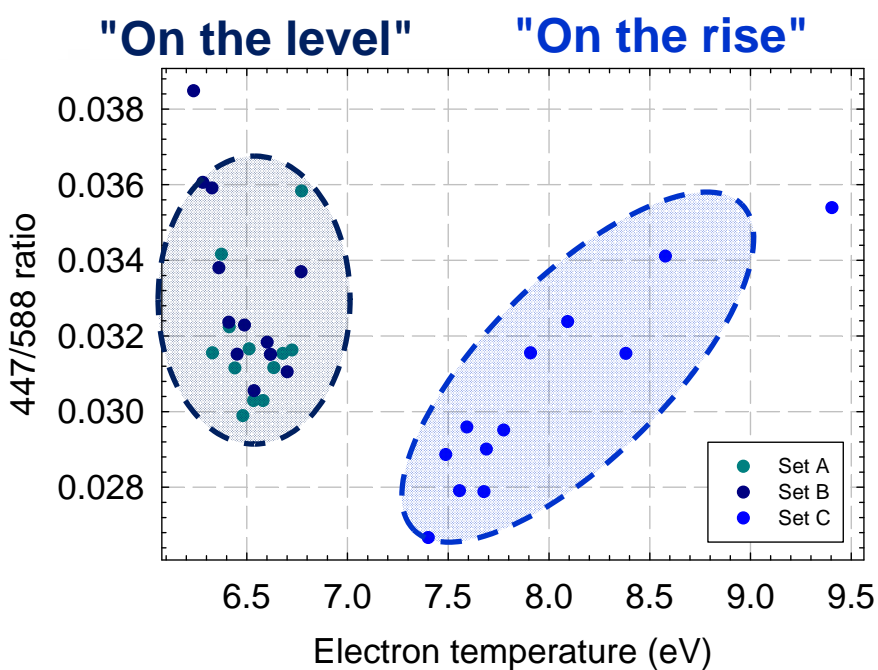
Averaged trends



Caution should still be used if considering the 3^3S state for normalization

[447]/[588] ratio captures trends but misses absolutes

- Anticipated T_e trends are observed
 - High temperature at start, low temperatures later on
- Measure T_e trends mimic computed trends
 - Discrepancy in absolute values are apparent



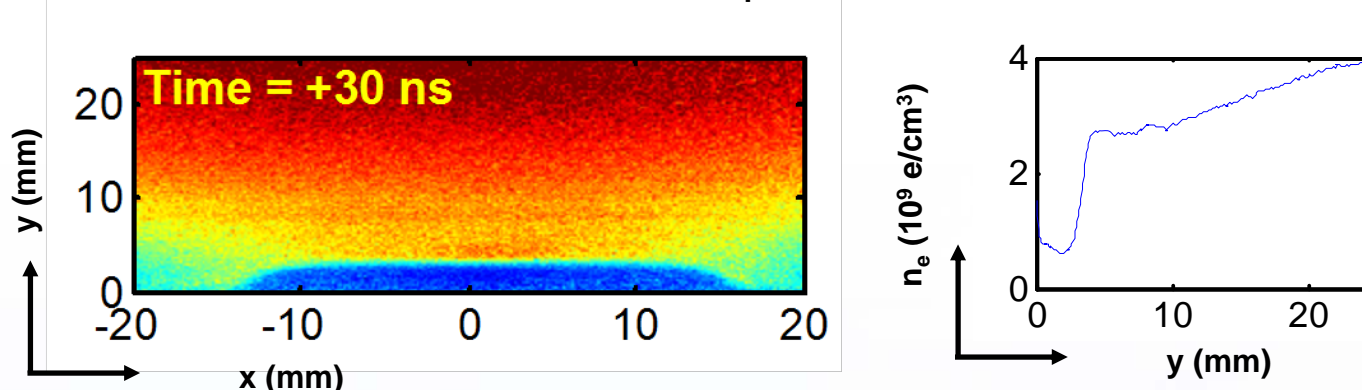
Uncertainties in rates, EEDF and/or interpolation of T_e from drift parameters should impact absolute values



Sandia National Laboratories

Analysis of ion-matrix sheath is used to further test LCIF technique

- Immediately after the pulse is applied
 - Electrons are rapidly pushed away from electrode
 - But ions should have little time to respond



- Using Poisson's equation and assuming quasi neutrality before the application of the pulse:

$$\nabla^2 V = \frac{e}{\epsilon_0} n \longrightarrow n_i \approx \frac{2\epsilon_0 V}{e \Delta x^2}$$

- For a voltage of 1 kV and a thickness of ~ 5 mm:

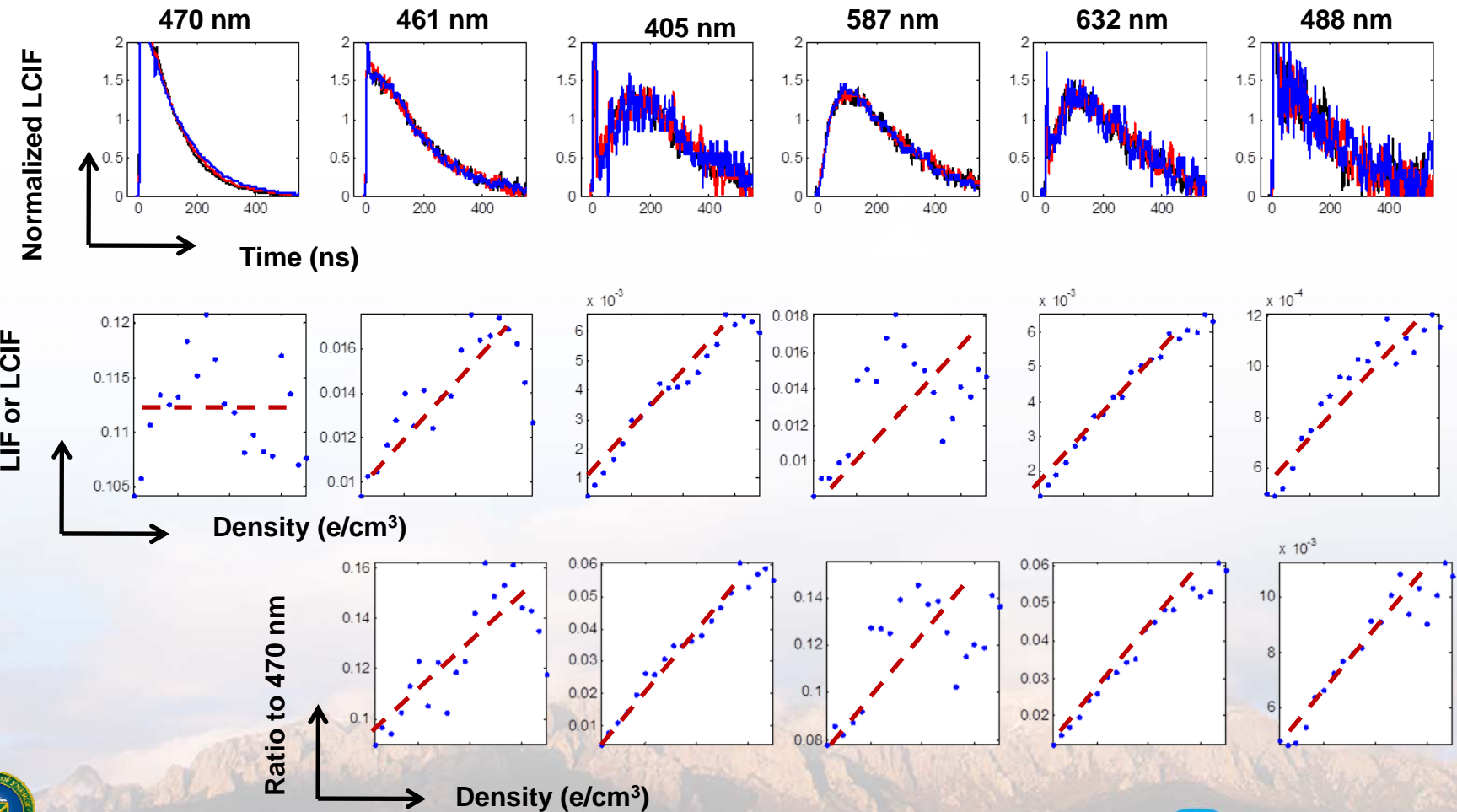
$$n_e \sim 4 \times 10^9 \text{ electrons/cm}^3$$

Reasonable cross-check of LCIF technique



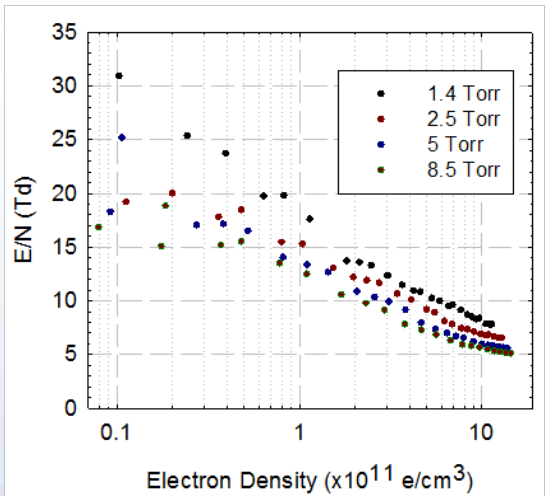
Sandia National Laboratories

Preliminary survey points to useful transitions

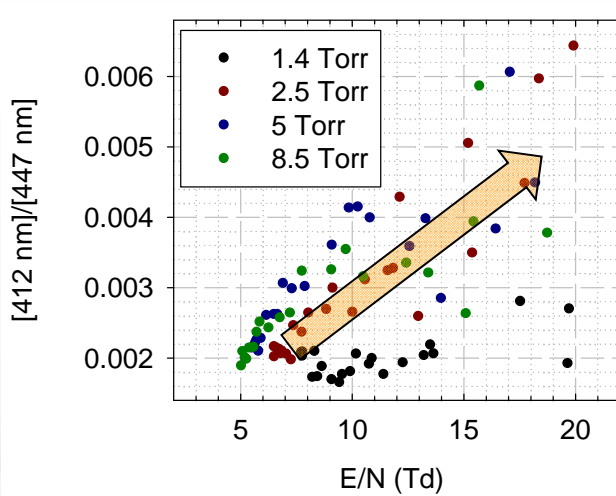


Preliminary investigation of proposed scheme looks promising

Extracted E/N



[412 nm]/[447 nm]



[403 nm]/[447 nm]

